8-2018

Synthesis and Characterization of Zinc(II) Dipyrrin Photosensitizers

Norah Alqahtani
East Tennessee State University

Synthesis and Characterization of Zinc(II) Dipyrrin Photosensitizers

---

A thesis

presented to

the Faculty of the Department of Chemistry

East Tennessee State University

In partial fulfillment

of the requirements for the degree

Master of Science in Chemistry

---

by

Norah Zarib Alqahtani

August 2018

Dr. Catherine E. McCusker

Dr. Marina Roginskaya

Dr. Cassandra T. Eagle

Keywords: Zinc(II) Dipyrrin Complexes, Photosensitizers, Triplet excited state

ABSTRACT

Synthesis and Characterization of Zinc(II) Dipyrrin Photosensitizers

by

Norah Zarib Alqahtani

Photocatalytic carbon dioxide reduction transforms CO_2 to useful chemicals and fuels, reducing CO_2 emissions and making fossil fuels more renewable. Due to a lack of earth-abundant sensitizers, we want to design new earth-abundant sensitizers to go with the many known carbon dioxide reduction catalysts. Zn(II) dipyrrin complexes strongly absorb visible light, but their excited state properties have not been widely studied. To investigate their photophysical properties, two Zn dipyrrin complexes, with and without heavy atoms, were synthesized and characterized by NMR and mass spectrometry. The photophysical properties of the two complexes were measured in polar and non-polar solvents, particularly fluorescence quantum yield and extinction coefficient. Also, through transient absorption spectroscopy, the triplet state quantum yield of both complexes was measures to determine the effect of solvent polarity and heavy atoms on the triplet state formation.

ACKNOWLEDGEMENTS

I am very grateful to my supervisor, Dr. Catherine McCusker, for her professional guidance in this research and for helping me in all the time of research and writing of this thesis. I would like to thank Dr. Cassandra T. Eagle and Dr. Marina Roginskaya for serving on my committee and for their advice on this work. I thank Dr. Phil Castellano and North Carolina State University for the use of the transient absorption instrument. I would also like to thank the faculty and staff of the Department of Chemistry ETSU.

I am thankful to my husband, family, and friends for their support, encouragement, prayer, and love during my studies. Finally, my sincere gratitude goes to my government for providing King Abdullah Scholarship Program and giving me the opportunity to complete my education.

TABLE OF CONTENTS

Page

ABSTRACT……..2

ACKNOWLEDGEMENTS……..……3

LIST OF TABLES……6

LIST OF FIGURES……..7

Chapter

1. INTRODUCTION……....10

Photocatalytic Reduction of CO_2……...12

Introduction to Emission Spectroscopy……15

Background Information of Homoleptic Zinc(II) Dipyrrins Complexes……..18

Complexes Including Iodine Ligand……23

Halogenated Boron Difluoride Dipyrrinato (BODIPY) Complex……24

Research Aims……..25

2. EXPERIMENTAL……...26

Materials……26

Solvents and Reagents……26

Methods……27

Bis (1, 3, 7, 9-tetramethyl-5-mesityldipyrrinato) Zinc(II) (ZnDPY) Synthesis…….27

Bis (2, 8- diiodo- 1, 3, 7, 9- tetramethyl-5- mesityldipyrrinato) Zinc(II) (ZnIDPY) Synthesis……31

Characterization of ZnDPY and ZnIDPY complexes…….……33

Nuclear Magnetic Resonance (NMR), Mass Spectrometry, and

Elemental Analysis……..……....33

Photophysical Properties of ZnDPY and ZnIDPY……...33

Extinction Coefficient Measurement ...……33

Photoluminescence Quantum Yield…….35

Transient Absorption……36

3. RESULTS AND DISCUSSION……..38

Synthesis and Characterization of ZnDPY and ZnIDPY …….38

ZnDPY Complex……38

ZnIDPY Complex……...41

Absorption Spectroscopy……...44

Emission Spectroscopy……..48

Transient Absorption…….52

4. CONCLUSION……56

Future Aims……..57

REFERENCES.....…….58

VITA.....……..65

LIST OF TABLES

Table Page

3.1. Table of ^{1}H-NMR signals and their assignments for ZnDPY complex in $CDCl_3$…….39

3.2. Table of ^{1}H-NMR signals and their assignments for ZnIDPY complex in $CDCl_3$……...42

3.3. Absorption properties of ZnDPY and ZnIDPY in toluene……..……..45

3.4. The photoluminescence quantum yield values of the two ZnDPY and ZnIDPY complexes in toluene and THF…….49

3.5. Triplet state extinction coefficient values of ZnDPY and ZnIDPY donor in toluene and THF……..54

3.6. Triplet state quantum yield values of ZnDPY in toluene and THF……...…….55

3.7. Triplet state quantum yield values of ZnDPY and ZnIDPY in THF……..……...55

LIST OF FIGURES

Figure Page

1.1. Estimated world fuel consumption in 2015……..……...…….10

1.2. Structure of a zinc(II) dipyrrins complex (left) and BODIPY complex (right)..……...11

1.3. The two pathways for photocatalysis with a reductive catalyst…….....……...14

1.4. Jablonski diagram…….....……..17

1.5. A series examples of symmetric zinc(II) dipyrrin complexes…….……...18

1.6. Example absorption spectra of a zinc(II) dipyrrin complex in different solvents.....19

1.7. A simplified Jablonski diagram illustrating the energy dependence of the charge separated (CS) state on solvent polarity…...……...……...….20

1.8. The structure of dipyrrin, showing IUPAC numbering…….....21

1.9. Aryl group in meso position in zinc(II) dipyrrin complex…….....23

1.10. A general structure of halogenated BODIPY dyes. Ar = Mes. X = Br,I……...…...24

2.1. Synthetic scheme for synthesizing 1, 3, 7, 9-tetramethyl-5-mesityldipyrromethane…….27

2.2. Synthetic scheme for dehydrogenating 1, 3, 7, 9-tetramethyl-5-mesityldipyrromethane.....……..28

2.3. Synthetic scheme for adding zinc(II) to 1, 3, 7, 9-tetramethyl-5-mesityldipyrromethene ligand……..…….…….....29

2.4. Synthetic scheme for adding iodine to 1, 3, 7, 9-tetramethyl-5-mesityldipyrromethene……...…….…….31

2.5. Synthetic scheme for adding zinc(II) to 2, 8- diiodo- 1, 3, 7, 9-

tetramethyl-5-mesityldipyrromethene……..…..……..32

2.6. A plot of absorption vs concentration to determine the extinction coefficient.....34

2.7. Different concentrations of ZnDPY and ZnIDPY complexes in toluene spectrophotometric grade.…..…….....35

3.1. Synthetic scheme for producing ZnDPY……...……....38

3.2. ^{1}H NMR of ZnDPY complex in $CDCl_3$…….....40

3.3. ^{13}C NMR of ZnDPY complex in $CDCl_3$……....40

3.4. Synthetic scheme for producing ZnIDPY…….....41

3.5. ^{1}H NMR of ZnIDPY complex in $CDCl_3$……...43

3.6. ^{13}C NMR of of ZnIDPY complex in $CDCl_3$…….....43

3.7. Absorption spectra of ZnDPY complex in toluene for different concentrations……..45

3.8. Example of a Beer's Law plot for ZnDPY in toluene…….....46

3.9. Absorption spectra of ZnIDPY complex in toluene for different concentrations….46

3.10. Example of a Beer's Law plot for ZnIDPY in toluene…….……...47

3.11. The extinction coefficients of the two ZnDPY and ZnIDPY in toluene……....47

3.12. Normalized emission of ZnDPY in toluene and THF……....49

3.13. Normalized emission of ZnIDPY in toluene and THF….……...50

3.14. Emission spectra of ZnDPY in toluene and standard $[Ru(bpy)_3]Cl_2$.....50

3.15. Emission spectra of ZnDPY in THF and standard $[Ru(bpy)_3]Cl_2$……...51

3.16. Emission spectra of ZnIDPY in toluene and standard $[Ru(bpy)_3]Cl_2$.……....51

3.17. Emission spectra of ZnIDPY in THF and standard $[Ru(bpy)_3]Cl_2$…….....52

3.18. Nanosecond transient absorption difference spectrum of (a) ZnDPY and (b) ZnIDPY in deaerated THF solution collected 50 μs after laser excitation.…....53

CHAPTER 1

INTRODUCTION

Almost 87% of the fuel in the world depends on fossil fuels like coal, petroleum, and natural gas.[1] The diminishing fossil fuel reserves and increasing levels of CO_2 in the atmosphere are serious problems. Increasing atmospheric levels of CO_2 cause anthropogenic global climate change and increasing average sea levels. The non-renewable nature of fossil fuels also makes their use unsustainable in the long term. Conversion of undesirable CO_2 to useful chemicals and new sources of energy provides a solution to both problems. Carbon dioxide reduction catalysis can recycle carbon dioxide into new fuel sources, which will make the use of petroleum fuels more sustainable. The transformation of carbon dioxide into fuel requires an input of energy, and the sun is an abundant source of energy; therefore, researchers are attempting to develop photocatalytic CO_2 reduction.[2,3]

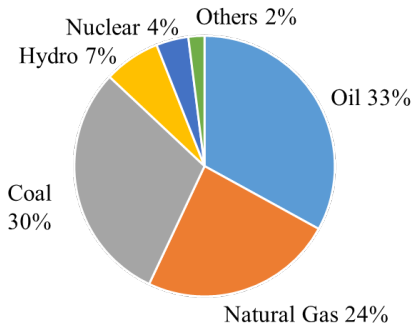

Figure 1.1. Estimated world fuel consumption in 2015[1]

Photocatalytic carbon dioxide reduction requires a photosensitizer, catalyst, and sacrificial electron donor. Complexes of the dipyrrin ligand have the potential to be good photosensitizers. Although boron dipyrromethene (BODIPY) complexes are the most

famous dipyrrin complexes, they are not a good candidates for bimolecular photosensitization due to their high fluorescence quantum yield which is a symptom of poor intersystem crossing (ISC) efficiency that leads to short excited state lifetimes.[4–7] Zinc(II) dipyrrin complexes are an alternative to the more used BODIPYs. While the photophysical properties of the zinc complexes are not as well studied as their BODIPY counterparts, there are a few examples where the formation of a long-lived triplet state has been spectroscopically observed.[8,9] However, it is still unknown what the quantum yield of that state is, and what factors affect that yield. Therefore, in this study the quantum yield of triplet state formation will be measured for two different Zn(II) dipyrrin complexes.

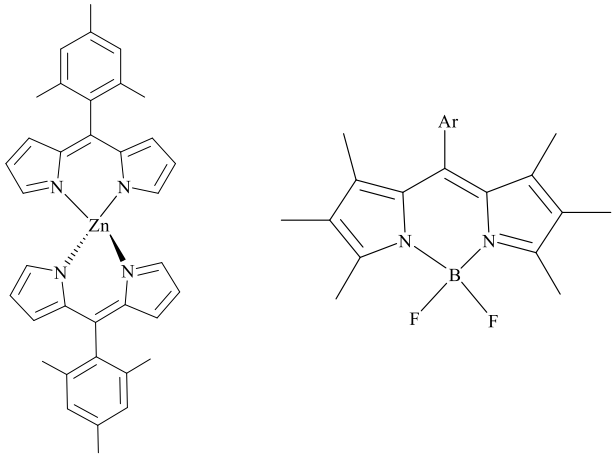

Figure 1. 2. Structure of a zinc(II) dipyrrin complex (left) and BODIPY complex (right)[6,9]

Dipyrrinato ligands are obtained by deprotonating dipyrrins which can work as monoanionic bidentate ligands for both main-group elements and transition metals. The first dipyrrinato complexes of transition metals were published in the early 1930s.[10] Recently, metal dipyrrinato complexes have received attention because of their potential applications in catalysis, metal-organic frameworks, light-harvesting arrays, coordination

polymers, and fluorescence.[11] There are a number of main-group dipyrrin-based molecules that have been synthesized and studied besides the abundant BODIPY class of complexes. Most of these complexes are homoleptic (symmetric) bis-or tris-dipyrrinato species with two or three identical dipyrrin ligands. Transition metals dipyrrinato complexes include homoleptic complexes of two or more identical ligands on a metal center. The most widely studied transition metal complexes of dipyrrin ligand are zinc(II) dipyrrins.[8,10–12]

Photocatalytic Reduction of CO_2

Conversion of CO_2 to useful chemicals by activation /reduction requires appropriate catalysts and energy input, and that poses essential challenges in chemical catalysis, electrochemistry, photochemistry, and semiconductor physics and engineering. CO_2 can be reduced to fuels such as methane and methanol or to fuel precursors such as CO/H_2 (synthesis gas). The reduction of CO_2 via proton-coupled multi–electron steps is more favorable than the single electron reduction, and more stable molecules are produced. This is illustrated in equations 1-5 (pH 7 in aqueous solution versus NHE under standard conditions). Because of reorganizational energy between the linear molecule and bent radical anion, the single electron reduction of CO_2 to $CO_2^{\bullet-}$ occurs at $E^o = -1.90V$.[2]

$$1\text{-}\ CO_2 + 2H^+ + 2e^- \longrightarrow CO + H_2O \quad E^0 = -0.53\ V \qquad (1-1)$$

$$2\text{-}\ CO_2 + 2H^+ + 2e^- \longrightarrow HCO_2H \quad E^0 = -0.61\ V$$

$$3\text{-}\ CO_2 + 4H^+ + 4e^- \longrightarrow HCHO + H_2O \quad E^0 = -0.48\ V$$

$$4\text{-}\ CO_2 + 6H^+ + 6e^- \longrightarrow CH_3OH + H_2O \quad E^0 = -0.38\ V$$

$$5\text{-}\ CO_2 + 8H^+ + 8e^- \longrightarrow CH_4 + 2H_2O \quad E^0 = -0.24\ V$$

$$6\text{-}\ CO_2 + e^- \longrightarrow CO_2^{\bullet-} \quad E^0 = -1.90\ V$$

The presence of a photosensitizer, a catalyst, and a sacrificial electron donor are the requirements for photocatalytic carbon dioxide reduction. A catalyst facilitates the chemical conversion from carbon dioxide to fuel, a photosensitizer absorbs light, and a sacrificial donor regenerates the sensitizer. Making the catalyst and photosensitizer from earth–abundant materials will make potential large-scale application of this technology more affordable in the future.[13–16] There are many known carbon dioxide reduction catalysts which contain first- row transition metals such as manganese[17–19], iron[13,20–22], cobalt[23–25], and nickel[26–28]. In contrast, the most commonly used photosensitizers are based on rare and expensive metals like iridium and ruthenium. Therefore there is a need for new photosensitizers derived from first-row transition metals. The advantages of using first-row metal complexes as sensitizers are that they are less costly and more earth abundant alternatives.[29]

A bimolecular system of sensitizer and catalyst has an advantage over covalently linked sensitizer-catalyst assemblies. In bimolecular systems, the detrimental electron transfer reaction from the catalyst back to the sensitizer is slow compared to covalently linked systems. That is important because the catalyst needs to be reduced multiple times to complete all of desirable transformations of CO_2 to fuel. A disadvantage of bimolecular photocatalysis is that the sensitizer must have long-lived excited state. Ideally, for efficient bimolecular reactions, the sensitizer should have an excited state lifetime longer than a microsecond. Before the excited sensitizer relaxes back to its ground state, it needs to diffuse through the solution and encounter a reaction partner. Triplet excited states meet this requirement because the relaxation back to the singlet

ground state is spin-forbidden, and therefore slow, resulting in a long-lived excited state.[29]

The most important criterion to design the sensitizers for photochemical carbon dioxide reduction is that the sensitizer must absorb visible light and should be soluble in the same environment that the carbon dioxide reduction is soluble in.[29] The lifetimes of the excited sensitizer should be sufficient to undergo electron transfer. The sensitizer should also be able to reduce the catalyst. The importance of the reversible electrochemistry is that the excited sensitizer can be oxidized or reduced and then regenerated for many cycles without decomposition, as illustrated in Figure1.3.

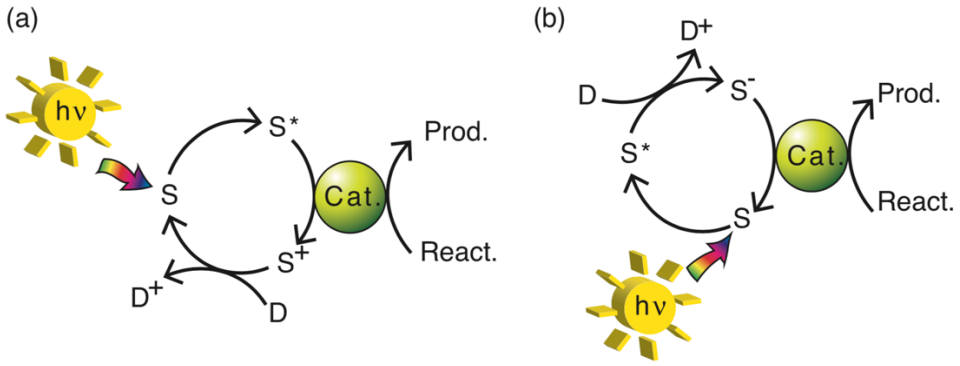

Figure 1.3. The two pathways for photocatalysis with a reductive catalyst (a) oxidative quenching pathway and (b) reductive quenching pathway. S indicates to the sensitizers and D represents the sacrificial electron donor

In the first mechanism for sensitization with a reductive catalyst, the catalyst can be oxidatively quenched by the excited sensitizer; this leads to oxidizing the sensitizer which can be regenerated by the sacrificial electron donor. In the second mechanism, the sacrificial electron donor can be reductively quenched by the excited sensitizer; this leads to reducing the sensitizer which can donate an electron to the sensitizer and return to the

ground state. With either the oxidative or reductive quenching mechanism, the excited sensitizer must be oxidized or reduced, then the oxidized or reduced sensitizer must undergo a second electron transfer reaction to return to the ground state.

Introduction to Emission Spectroscopy

Luminescence, the emission of light from molecules, is closely associated with the absorption of light by molecules. When a molecule absorbs a photon of visible light, an electron is transferred from one orbital to a higher-energy orbital, making it in an excited state. This excited state species quickly relaxes to the lowest vibrational energy state of the electronic excited state, and for many pathways, this excited state can relax back to the singlet ground state, S_0. These pathways include internal conversion (IC), ISC to a triplet excited state, energy transfer to an acceptor species, and emission of a photon of a lower energy than the absorbed photon (Figure 1.4).[12] Luminescence is called phosphorescence when the spin of the excited state is different from the ground state. Fluorescence occurs when a photon is emitted directly from the singlet excited state (S_n, $n \geq 1$). The efficiency of luminescence emission is described by the emission quantum yield Φ.

$$\Phi = \frac{number\ of\ photons\ emitted}{number\ of\ photons\ absorbed} \qquad (1-2)$$

The difference in energy between the absorption and emission of the photon is also described by the emission, and this is known as the Stokes shift. Most luminescent molecules are rigid and conjugated species. The conjugated oligopyrroles like dipyrrin are luminescent and meet this criterion. The emission quantum yield increases as the rigidity of a luminophore of any structure increases. That is achieved in oligopyrroles

such as dipyrrin by the extension of the π-system by the introduction of bulky meso-aryl-substituents which helps to restrict rotation the C_{meso}- C_{aryl} bond. A large Stokes shift more than 150 nm and long excited-state lifetimes are what characterize phosphorescence. [30] The quantum yields of phosphorescence are significantly lower than the fluorescence because of the long lifetimes and non-radiative relaxation pathways become kinetically competitive with photon emission. The introduction of heavy atoms into the structure of the oligopyrrole complex like dipyrrin enhances the phosphorescence. Heavy atoms can also enhance spin-orbit coupling which increases the probability of intersystem crossing and raises the potential of $T_n \rightarrow S_0$ phosphorescence.[30] This is observed in oligopyrrole systems that are linked to second- and third- row transition metals.[12] Heavy halogens like bromine and iodine enhance spin-orbit coupling and phosphorescence emission, but this has not been widely studied in oligopyrrole complexes. [12,31]

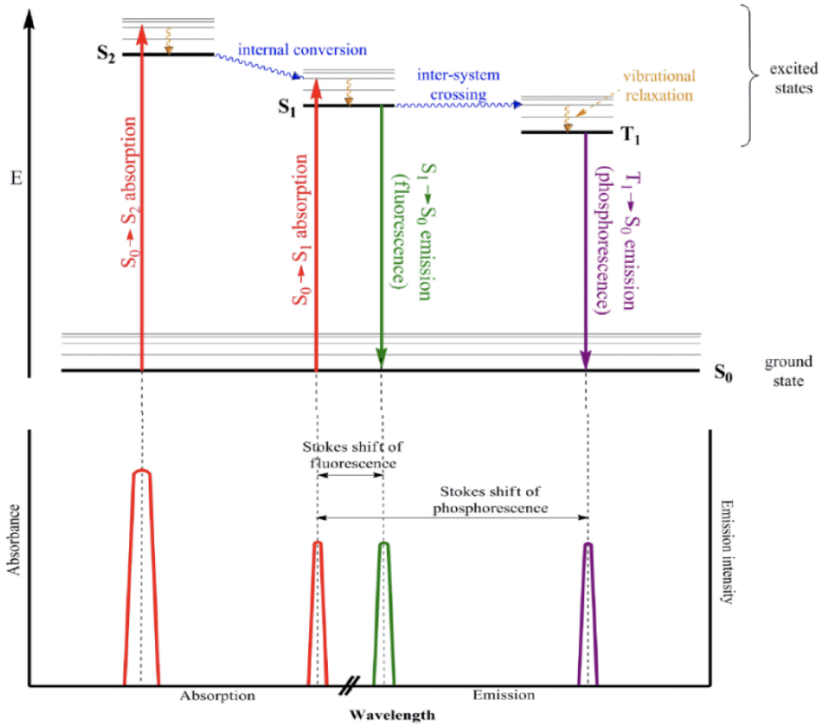

Figure 1.4. Jablonski diagram (top part) illustrating absorption (red), fluorescence emission (green), and phosphorescence emission (purple), and connecting with absorption and emission spectra (bottom part). Non-radiative pathways of relaxation to the ground state include vibrational relaxation, internal conversion, and inter-system crossing. Gray lines illustrate vibrationally excited states within a given electronic state[12]

Background Information of Homoleptic Zinc(II) Dipyrrins Complexes

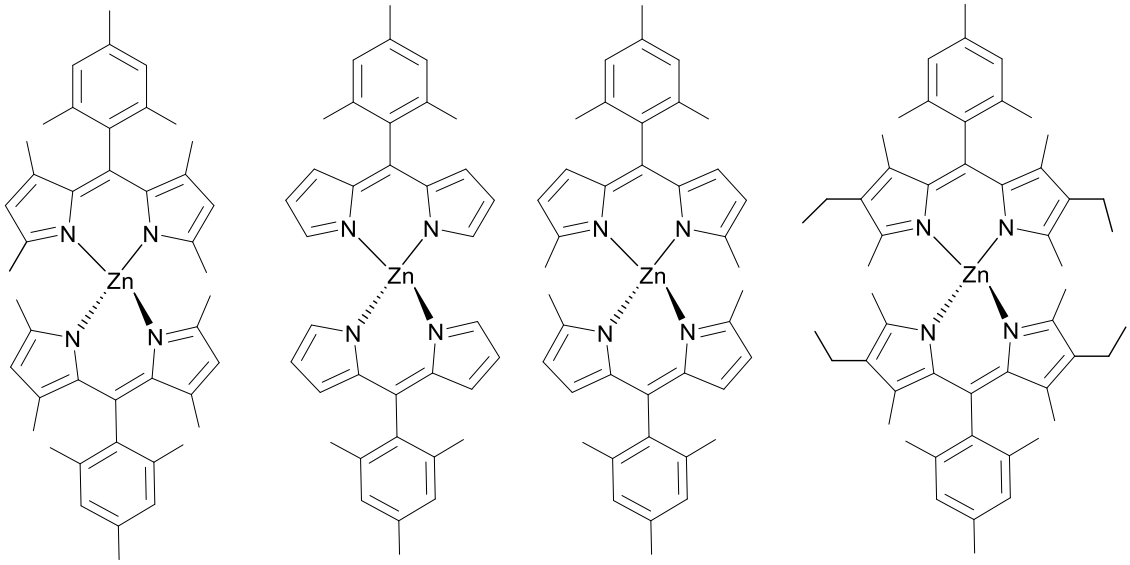

Figure 1.5. A series examples of symmetric zinc(II) dipyrrin complexes from published literatures[8,9]

The photophysics of zinc dipyrrin complexes shows strong visible absorption in a variety of organic solvents.[8] Small changes in dipyrrin structure can have a large effect on the absorption wavelength. For the four complexes in Figure 1.5, the absorption maximum shifts by ~20 nm. The rigid structure of zinc(II) dipyrrin complex shows emission with a fluorescence quantum yield (Φ_F) of 0.36 in toluene. Antina and colleagues found out that the fluorescence quantum yield (Φ_F) reaches 0.91 in cyclohexane for double-helical bis(dipyrrinato)zinc(II) complexes.[10] Zinc(II) dipyrrin complexes can be either homoleptic (two identical dipyrrin ligands) or heteroleptic (two different dipyrrin ligands). Homoleptic zinc(II) dipyrrin complexes showed a lower fluorescence quantum yield than the heteroleptic complexes, and that is due to the low fluorescence quantum yields for dipyrrin or π- extended dipyrrin ligands. Symmetric

zinc(II) dipyrrin complexes are luminescent but exhibited only weak photoluminescence PL (Φ_{PL}= 0.03-0.21) in nonpolar toluene.[32] The electrochemical properties of the symmetric zinc(II) dipyrrin complexes were studied by cyclic voltammetry to examine the energy levels of the π and π^* orbitals of the dipyrrinato ligands. The molecular orbitals of zinc(II) dipyrrin complexes were calculated with density functional theory (DFT), and their energy levels were determined from electrochemical measurements.[32]

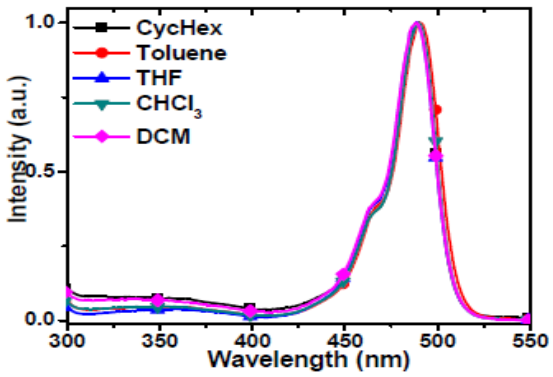

Figure 1.6. Example absorption spectra of a zinc dipyrrin complex in different solvents [9]

Homoleptic zinc(II) dipyrrin complexes have two identical dipyrrin ligands, and they have tetrahedral geometry as heteroleptic zinc(II) dipyrrin complexes which is important to forming the charge separated state (CS). These complexes show high fluorescence quantum yields in nonpolar solvents and strongly absorb at 450-550 nm. In contrast, the emission in polar solvents is weak to nonexistent. The fluorescence quantum yield decreases in polar solvents because the CS state is stabilized in polar solvents and becomes lower in energy than the fluorescent singlet excited state (S_1) and formation of the CS state becomes favorable. When zinc(II) dipyrrin complexes have two dipyrrin ligands they can form a CS state by intramolecular electron transfer between the two dipyrrins where one of the ligands is oxidized and the other is reduced. The CS is non-

emissive and possibly forms the excited triplet state (T_1) which is localized on a single ligand. The T_1 state can be phosphorescent at 77 K, but is usually not at room temperature.[9]

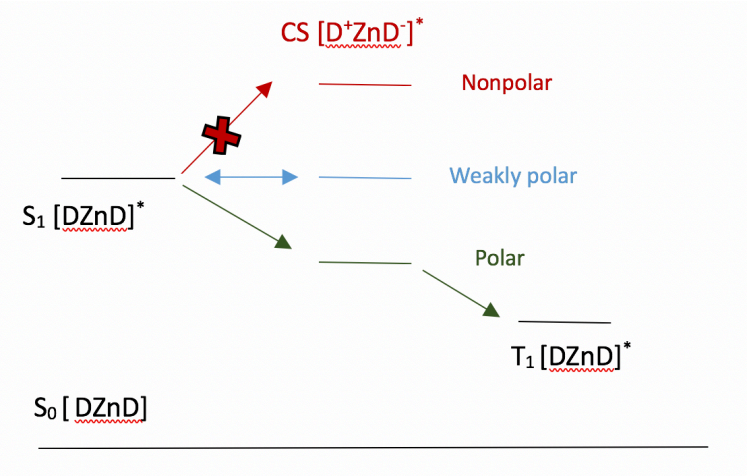

Figure 1.7. A simplified Jablonski diagram illustrating the energy dependence of the CS state on solvent polarity[9]

In polar solvents, the CS state quenches the first excited singlet state S_1. The fluorescence properties of zinc(II) dipyrrin complexes are strongly solvent-dependent because of the presence of the CS state. The CS state is stable in polar solvents, and it is lower energy than the first excited state S_1. Thus, the formation of the CS state by intramolecular electron transfer is competitive with the radiative decay from the S_1 state. At room temperature, the T_1 of zinc(II) dipyrrin complexes is non-emissive, but it has been observed in solution by transient absorption spectroscopy.[9] The formation of the T_1, which is the accepted way for zinc(II) dipyrrin complexes to go from the first formed S_1 state to the T_1, is not a direct ISC, but instead of that, in polar solvents, the CS state is an intermediate state.[8,9,32]

The single crystal X-ray structures of the zinc(II) dipyrrin complexes were studied and it was shown that the length of the Zn-N bond in zinc dipyrrin complexes ranges from 1.95 to 1.99 Å. The zinc center takes a distorted tetrahedral configuration with two ligands grasped almost perpendicular to each other. The dihedral angles between the two dipyrrin ligands are 76.7°. Symmetric zinc(II) dipyrrin complexes in polar solvent undergo charge separation and thus show an efficient nonradiative pathway for electronic excited states. However, these complexes in nonpolar solvents do not undergo charge separation and therefore show higher quantum yields than dissymmetric zinc(II) dipyrrin complexes. This ability of zinc(II) dipyrrin complexes to undergo charge separation make them a new source for use in organic photovoltaics. [9]

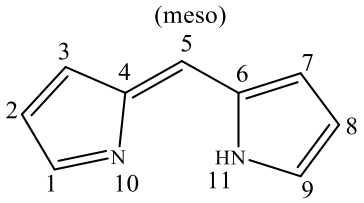

Figure 1.8. The structure of dipyrrin, showing IUPAC numbering[10]

The dipyrrin ligand has two pyrrole units connected by a sp^2 carbon atom, and it is a monovalent bidentate ligand. Dipyrrins are a group of π- conjugated organic molecules with high absorption in the visible region. Pyrrolic nitrogen atoms in dipyrrins have the ability to coordinate to metals.[8,11] Dipyrromethenes, pyrromethenes, and dipyrrylmethenes are also known as dipyrrins. The electronic and geometric specifications of dipyrrins can reflect the similarity as hemi-porphyrins. Dipyrrins are versatile compounds due to their strength, special properties (absorptivity and

luminescence), ease of synthesis, and highly variable structure. The flexibility to link metals in geometries and the ability to functionalize the 1 to 9 positions of dipyrrins are also two features that specialize dipyrrins. The stability of a dipyrrin is affected by the number and kind of substituents. Unsubstituted dipyrrin is unstable in solution because of the susceptibility of the unsubstituted positions in dipyrrin ring to nucleophilic and electrophilic attack. Alkyl substituents on the pyrrole rings promote the stability of the dipyrrin. When the aryl substituents are at the 5-position in dipyrrins and 1, 2, 3, 7, 8, 9-positions are unsubstituted, the stability of dipyrrins increases as the stability of radical cations formed from dipyrrin increase and that makes the 5- substituted dipyrrins more appropriate for optoelectrochemical applications than 5- unsubstituted dipyrrins. Isolable complexes with a variety of metal ions can form from dipyrrins by deprotonation of the monoanionic dipyrrinato ligands which usually, but not always, form neutral homoleptic complexes that carry two or more identical ligands on a metal center. Zinc(II), nickel(II), copper(II), cadmium(II), magnesium(II), calcium(II), and iron(II) form complexes of this type.[10]

Metal dipyrrinato complexes exhibit two intense absorption bands in the visible region of the electromagnetic spectrum. The ligand with $\pi \rightarrow \pi^*$ transitions has more intense absorption than the corresponding free dipyrrins due to the rigidification of the π- system by chelation to the metal atom. The ligand with lower energy $\pi \rightarrow \pi^*$ transitions has less intense of these absorptions, and it is blue-shifted from the free dipyrrin absorption band. These transitions are referred to closely-spaced $S_0 \rightarrow S_2$ and $S_0 \rightarrow S_1$ transitions for the ligand-based π- systems, where S_0 symbolizes the singlet ground state and S_1 and S_2 symbolize singlet excited states.[12]

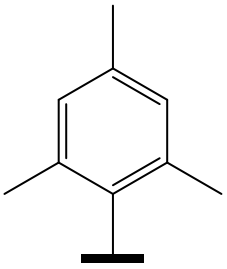

Figure 1.9. Aryl group in meso position in zinc(II) dipyrrin complex[11]

The meso-aryl groups of the bis dipyrrinato zinc(II) complexes have a small impact on the ground and photoexcited electronic states of the dipyrrin subunit. The identity of the meso-aryl group in the excited state strongly affects the accessibility of nonradiative pathways. Moreover, the meso- aryl groups have a great effect on the fluorescence quantum yields. At the meso-position on the dipyrrin ligand rotation, the phenyl ring is the reason for nonradiative deactivation of the excited state, so inserting more bulky mesityl substituent instead of phenyl will inhibit this rotation and improve the fluorescence quantum yield of bis (dipyrrinato) zinc(II) complexes.[9,11,32–35]

Complexes Including Iodine Ligand

The addition of iodine atoms in boron dipyrrin complexes (BODIPYs) has enhanced the ISC between S_1 and T_1 states, so we hypothesize that the addition of iodine will enhance the ISC between the CS and T_1 states in zinc(II) dipyrrin complexes.[22,23,36,37] The ligand substitution with iodine does not affect the intensity of the [ML_2] electron absorption as compared with the previously studied alkyl derivatives of dipyrrolylmethenates. As compared with the alkyl-substituted dipyrrolylmethenates, the

ligand substitution with a heavy iodine atom decreases the thermal stability of the prepared complexes. The iodosubstituted dipyrromethene [ZnL_2] are interesting fluorophores that show a set of important properties.[38]

Halogenation of dipyrrins has an impact on absorption λ_{max} because resonance and inductive effects play a role in the π-system. The electron withdrawing halogen removes electron density from the dipyrrin π-system, decreases the energy gap between the HOMO and LUMO orbitals resulting in red-shifted absorption and emission.[12]

Halogenated Boron Difluoride Dipyrrinato (BODIPY) Complex

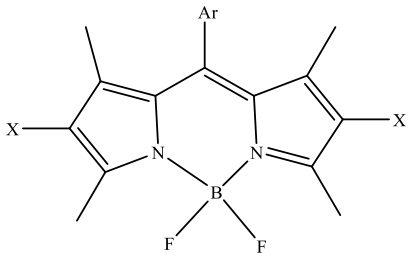

Figure 1.10. A general structure of halogenated BODIPY dyes. Ar = Mes. X = Br,I [37]

Adding halogens such as Br and I in BODIPY causes the absorption and emission energies to shift to lower energy, and both quantum yields and fluorescent lifetimes decrease. By adding halogens in BODIPY, the optimized geometry does not significantly change. The iodinated derivative in BODIPY worked as photosensitizers for the photoreduction of water.[37] The rate of the ISC from the first excited π-π^* state increases by iodination of BODIPY chromophores, and that generates greater contribution of the π-π^* state. Shifting the absorption and emission spectra to lower energy for the halogenated BODIPY reflects changes in the energies of the LUMO and HOMO and that was proved by electrochemistry. The DFT calculations are in agreement with the

electrochemistry. The halogenated BODIPY shows that both frontier orbitals decrease in energy and probably stabilize by the electron withdrawing nature of the halogens. Only halogenated dyes are active because of their long-lived excited triplet states. When the BODIPY dye contains iodine substituents, it is effective for the light-driven generation of H_2. The oxidation potentials of halogenated BODIPY are more positive than the original compounds whereas the reduction potentials of the halogenated BODIPY are less negative due to the effect of the electron withdrawing of the halogen substituents. Therefore, the electronegative halogens make BODIPY core more electron deficient. [37]

Research Aims

The aims of this research are:

1. To synthesize zinc(II) dipyrrin complex (ZnDPY) and the new zinc(II) iodine dipyrrin complex (ZnIDPY).
2. To characterize the two complexes using NMR, mass spectroscopy, and elemental analysis.
3. To measure the photophysical properties of the two complexes, particularly extinction coefficient and fluorescence quantum yield in both polar and non-polar solvents.
4. To qualitatively identify triplet state formation for the two ZnDPY and ZnIDPY complexes using nanosecond transient absorption.
5. To quantify the yield of triplet state formation in polar and non-polar solvents by comparison to known standards.

CHAPTER 2
EXPERIMENTAL

Materials

Solvents and Reagents

1. Acetone [$(CH_3)_2CO$]
2. Aluminum oxide (alumina)
3. Anhydrous sodium sulfate (Na_2SO_4)
4. Chloroform ($CHCl_3$)
5. Chloroform-d ($CDCl_3$)
6. Coarse sand
7. Deionized water (H_2O)
8. Dichloromethane (methylene chloride) (CH_2Cl_2)
9. 2,3-dichloro-5,6-dicyano-1,4-benzoquinone (DDQ)
10. 2,4-Dimethylpyrrole
11. Hexane [$CH_3(CH_2)_4CH_3$]
12. Iodic acid (HIO_3)
13. Iodine
14. Mesitaldehyde ($C_{10}H_{12}O$)
15. Methanol (CH_3OH)
16. Sodium bicarbonate ($NaHCO_3$)
17. Sodium carbonate (Na_2CO_3)
18. Sodium sulfite (Na_2SO_3)
19. Tetrahydrofuran (THF) [$(CH_2)_3CH_2O$]
20. Tetrahydrofuran, spectrophotometric grade, >99.7%

21. Toluene [$CH_3(C_6H_5)$]

22. Toluene, spectrophotometric grade , ≥99.5%

23. Triethylamine [$(C_2H_5)_3N$]

24. Trifluoroacetic acid (TFA) (CF_3COOH)

25. Zinc acetate dihydrate [$Zn(O_2CCH_3)_2 \bullet 2H_2O$]

Methods

Bis (1, 3, 7, 9-tetramethyl-5-mesityldipyrrinato) Zinc(II) (ZnDPY) Synthesis

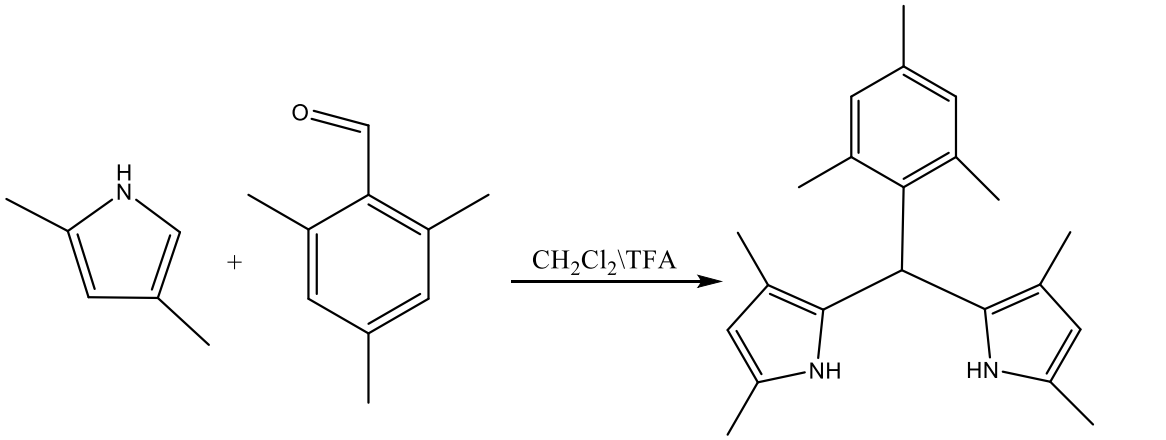

Figure 2.1. Synthetic scheme for synthesizing 1, 3, 7, 9-tetramethyl-5-mesityldipyrromethane

The synthesis of bis (1, 3, 7, 9-tetramethyl-5-mesityldipyrrinato) zinc(II) complex was accomplished through the method described by Thompson and colleagues with few changes discussed below.[9] 1, 3, 7, 9-tetramethyl-5-mesityldipyrromethane was synthesized from 2-4 dimethylpyrrole and mesitaldehyde. 2-4 dimethylpyrrole (1.56 mL, 15.13 mmol) and (1.14 mL, 7.75 mmol) mesitaldehyde were dissolved in 50 mL of

dichloromethane, and 1 drop of trifluoroacetic acid (TFA) was added to the stirred solution under nitrogen. After stirring for 6 h, 0.75 mL of triethylamine was added to quench the reaction. The reaction mixture was washed with a saturated aqueous solution of Na_2CO_3 (25 mL, 3 times) and brine (25 mL, 1 time), and it was dried over anhydrous Na_2SO_4. The solvent was removed under reduced pressure. The final product was a viscous dark yellow-green liquid which solidified upon standing at room temperature. Total yield was 2.31 g (95%). The NMR spectrum of the product 1, 3, 7, 9-tetramethyl-5-mesityldipyrromethane matched reported values and used for the next step without further purification.

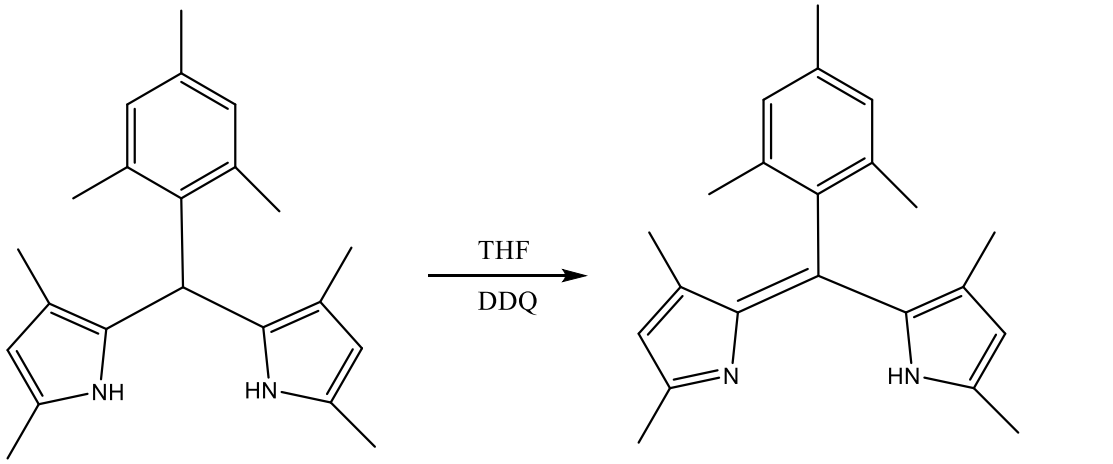

1, 3, 7, 9-tetramethyl-5-mesityldipyrromethane

1, 3, 7, 9-tetramethyl-5-mesityldipyrromethene

Figure 2.2. Synthetic scheme for dehydrogenating 1, 3, 7, 9-tetramethyl-5-mesityldipyrromethane

2.31 g of the solid 1, 3, 7, 9- tetramethyl-5-mesityldipyrromethane was dissolved in 62.5 mL freshly distilled tetrahydrofuran (THF), and a solution of 2,3-dichloro-5,6-dicyano-1,4-benzoquinone (DDQ) (1.7567 g, 7.73 mmol) in 8.75 mL of THF was added slowly to the stirred 1, 3, 7, 9- tetramethyl-5-mesityldipyrromethane solution under nitrogen. After

stirring under nitrogen for 1 h, the reaction was quenched with 2.5 mL of triethylamine and left for one day under nitrogen. The solvent was then removed under reduced pressure, and the product obtained was dissolved in 125 mL of dichloromethane. The mixture was then washed with saturated $NaHCO_3$ solution (3 times) and brine (1 time). The solution was dried by anhydrous Na_2SO_4 and filtered. The NMR spectrum of the product 1, 3, 7, 9-tetramethyl-5-mesityldipyrromethene matched reported values and was used for the next step without purification.

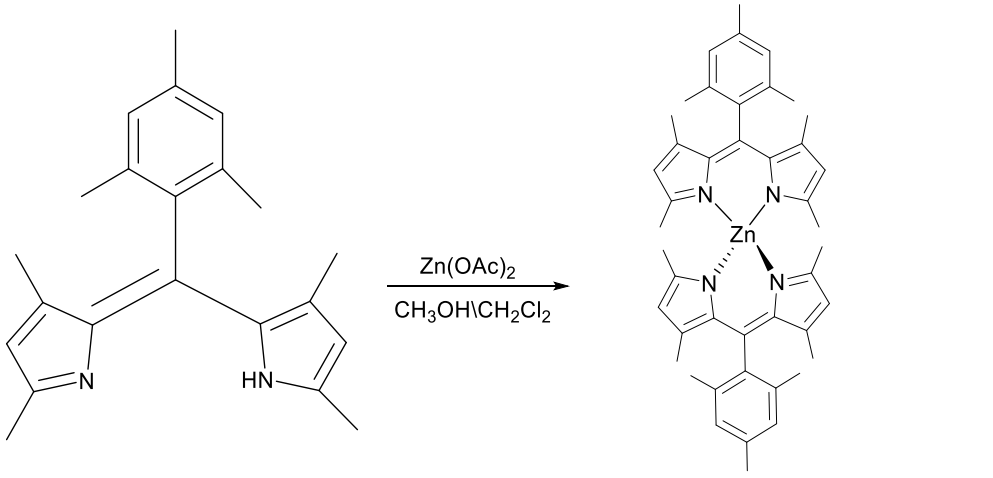

1, 3, 7, 9-tetramethyl-5-mesityldipyrromethene

Bis (1, 3, 7, 9-tetramethyl-5-mesityldipyrrinato) zinc (II) complex

[ZnDPY]

Figure 2.3. Synthetic scheme for adding zinc(II) to 1, 3, 7, 9-tetramethyl-5-mesityldipyrromethene ligand

A solution of zinc acetate dihydrate ($Zn(OAc)_2 \bullet 2H_2O$) (5.13 g, 23.371 mmol) in 25 mL of methanol was prepared and added to the solution of 1, 3, 7, 9-tetramethyl-5-mesityldipyrromethene in dichloromethane. The reaction mixture was left under air and stirred overnight. After that, the solution was filtered using filter paper, and the solvents

were removed under reduced pressure yielding a dark green solid. The solid was dissolved in a mixture of hexane/dichloromethane (7/3 v/v) and passed through a short neutral alumina plug using the same mixture as eluent. Then, the orange-red portion was collected, and the solvents were removed under reduced pressure. The solid was recrystallized from CH_2Cl_2/MeOH, and purified by sublimation under vacuum at temperature between 180 °C – 200 °C. The yield of bis (1, 3, 7, 9-tetramethyl-5-mesityldipyrrinato) zinc(II) complex was orange-red in powder form and dark green as crystals possibly because of intermolecular interactions in the crystal 414.2 mg (8 % total yield). Total yield implies that is the yield for the whole synthetic procedure, not just this step. ^{1}H NMR (400 MHz, $CDCl_3$): δ ppm 6.92 (s, 4H), 5.90 (s, 4H), 2.34 (s, 6H), 2.10 – 2.02 (s, 24H), 1.29 (s, 12H). ^{13}C NMR (100 MHz, $CDCl_3$): δ ppm 155.99, 143.73, 143.24, 137.44, 136.28, 135.63, 134.61, 128.83, 119.63, 21.30, 19.33, 16.20, 14.91. EA Calcd for $C_{44}H_{50}N_4Zn$. 1.05 H_2O: C, 72.62%; H, 7.43%; N, 8.00% found C,72.66%; H, 7.33%; N,7.50%. HRMS (ESI) Calcd for $C_{44}H_{50}N_4Zn$ 699.3398 $[M-H]^+$, Found: 699.3405 $[M-H]^+$.

Bis (2, 8- diiodo- 1, 3, 7, 9- tetramethyl-5- mesityldipyrrinato) Zinc(II) (ZnIDPY)

Synthesis

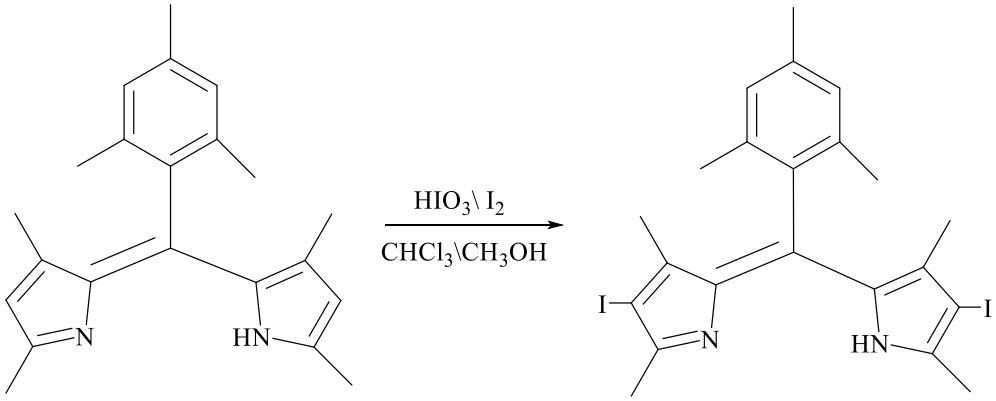

1, 3, 7, 9-tetramethyl-5-mesityldipyrromethene

2, 8- diiodo- 1, 3, 7, 9- tetramethyl-5-mesityldipyrromethene

Figure 2.4. Synthetic scheme for adding iodine to 1, 3, 7, 9-tetramethyl-5-mesityldipyrromethene

The synthesis of 2, 8- diiodo- 1, 3, 7, 9- tetramethyl-5- mesityldipyrromethene (IDPY) was accomplished through the method described by Sakamoto and colleagues.[32] 1, 3, 7, 9-tetramethyl-5-mesityldipyrromethene (639.6 mg, 2 mmol), chloroform/methanol 1:1 v/v solution (80 mL), iodine (1025.3 mg, 4 mmol), and an aqueous solution (10 mL) of iodic acid (706 mg, 4mmol) were stirred for one hour at room temperature. After 1 h, the solution was diluted with chloroform (200 mL) and washed with an aqueous solution of sodium sulfite (10 g) and sodium bicarbonate (2 g) in 200 mL of water. The reaction mixture was dried over anhydrous sodium sulfate, and the solvents were removed under reduced pressure. Total yield was 943.9 mg of red brown powder. The NMR of the crude solid matched that reported in the literature, and the solid was used without further purification. ^{1}H NMR (400 MHz, $CDCl_3$): δ ppm 6.91 (s, 2H), 2.40 – 2.34 (s, 9H), 2.04 (s, 6.36H), 1.28 (s, 6.57H).

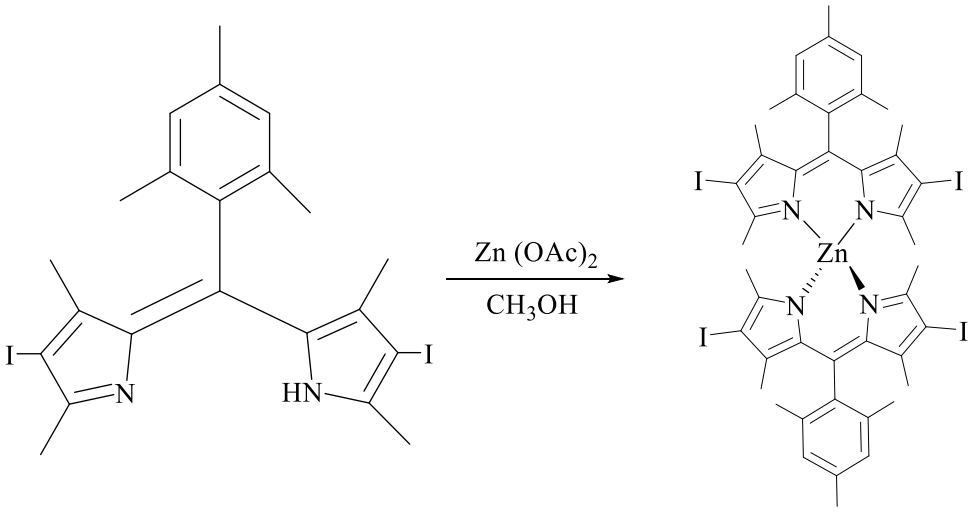

2, 8- diiodo- 1, 3, 7, 9- tetramethyl-5- mesityldipyrromethene

Bis (2, 8- diiodo- 1, 3, 7, 9- tetramethyl-5- mesityldipyrrinato) zinc (II) complex [ZnIDPY]

Figure 2.5. Synthetic scheme for adding zinc(II) to 2, 8- diiodo- 1, 3, 7, 9- tetramethyl-5- mesityldipyrromethene

Zinc(II) 2, 8- diiodo- 1, 3, 7, 9- tetramethyl-5- mesityldipyrromethene was synthesized by following the method that was described by Dudina and colleagues with changes discussed below.[39] 2, 8- diiodo- 1, 3, 7, 9- tetramethyl-5- mesityldipyrromethene (398.4 mg, 0.698 mmol) was dissolved in methanol (7 mL) and mixed with a solution of zinc acetate dihydrate ($Zn(OAc)_2 \bullet 2H_2O$) (306.4 mg, 1.4 mmol) in 4 mL methanol. Triethylamine, 0.097 mL, was added to the reaction mixture, and the solution was stirred at room temperature overnight. The precipitated complex was filtered. The solid was dissolved in dichloromethane and passed through a short neutral alumina plug using dichloromethane as eluent. Then, the orange-red portion was collected, and the solvents were removed under reduced pressure. The obtained solid was recrystallized from CH_2Cl_2/MeOH. The yield of bis (2, 8- diiodo- 1, 3, 7, 9- tetramethyl-5- mesityldipyrrinato) zinc(II) complex was 48.8 mg (2.90 %) of a dark green solid.

Satisfactory EA results were not obtained. Complex identity and purity was determined by ^{1}H and ^{13}C NMR and HRMS. ^{1}H NMR (400 MHz, $CDCl_3$): δ ppm 6.95 (s, 4H), 2.36 (s, 6.5H), 2.10 – 2.05 (s, 24.8H), 1.31 (s, 12.2H). ^{13}C NMR (100 MHz, $CDCl_3$): δ ppm 157.27, 145.46, 144.43, 138.53, 135.97, 135.51, 135.02, 129.44, 84.02, 29.94, 21.50, 19.55, 17.67, 17.49. HRMS (ESI) Calcd for $C_{44}H_{46}I_4N_4Zn$ 1201.9187 [M+], Found: 1201.9193 [M+].

Characterization of ZnDPY and ZnIDPY complexes

Nuclear Magnetic Resonance (NMR), Mass Spectrometry, and Elemental Analysis

NMR data for IDPY ligand and two ZnDPY and ZnIDPY complexes were collected using a JOEL AS400 FT-NMR spectrometer. For each experiment about 3 mg of the obtained solid was dissolved in $CDCl_3$ and pipetted into the NMR tube for data collection. The high-resolution electrospray ionization mass spectroscopy (HR ESI-MS) of the two ZnDPY and ZnIDPY complexes was performed in the Michigan State University Mass Spectrometry & Metabolomics Core. Approximately 6 mg of purified ZnDPY and ZnIDPY complexes were sent to Atlantic Microlab, Inc. Analysis was requested for carbon, hydrogen, and nitrogen to prove the purity and confirm NMR data of the two complexes. The data of the lab analysis was given in percent by mass.

Photophysical Properties of ZnDPY and ZnIDPY

Extinction Coefficient Measurement

The relationship between absorbance and concentration is determined by the extinction coefficient. UV-Vis spectroscopy is used to measure absorbance of light of a

specific wavelength. The extinction coefficient can be measured according to Beer's Law as shown in equation (2 – 1)[40] where the slope of the graph from a linear regression of the data at the chosen wavelength represents the extinction coefficient, as illustrated in Figure 2.6.

$$A = \varepsilon L c \qquad (2 - 1)$$

In this equation, A is the absorbance of the sample, ε is the extinction coefficient at the specific wavelength, c represents the concentration of the species in the sample, and L is the path length of the cuvette.

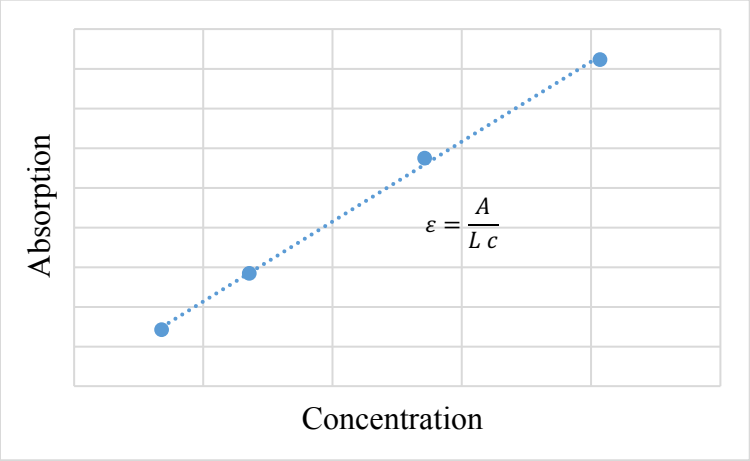

Figure 2.6. A plot of absorption vs concentration to determine the extinction coefficient. Slope corresponds to the extinction coefficient

Figure 2.7. Different concentrations of ZnDPY (left) and ZnIDPY (right) complexes in toluene spectrophotometric grade for measuring the extinction coefficient

1 mg of each pure complex was dissolved in 100 mL of spectrophotometric grade (≥99.5%) toluene. The solution was divided into 4 different (10 mL) volumetric flasks with different concentrations for sample 1, 2 mL, sample 2, 4 mL, sample 3, 6 mL, and sample 4, 8 mL and the remaining part of every flask was filled with toluene. The absorbance of every sample was measured by UV-Vis spectroscopy. The plot of absorbance versus concentration has showed linear regression, and the calculated slope represented the extinction coefficient.

Photoluminescence Quantum Yield

Emission spectra were collected with an FS5 fluorometer (Edinburgh Instruments) equipped with a 150 W Xe arc lamp excitation source and a PMT (R928P, Hamamatsu) detector. All emission spectra were corrected for detector response. Quantum yields for the complexes were measured relative to aerated $[Ru(bpy)_3]Cl_2$ in water ($\Phi = 0.040$).[41] For each measurement, optically dilute (Abs = 0.1−0.2) solutions were prepared in air

equilibrated, spectrophotometric grade toluene or THF and were excited at 475 nm for ZnDPY complex and 500 nm for ZnIDPY complex. The absorption of the unknown and standard samples were measured by UV-Vis spectrophotometer. The refractive index was known from handbook of photochemistry for toluene, THF and H_2O, respectively 1.49693, 1.40716 and 1.33299.[42] From these data the photoluminescence quantum yield of the sample can be calculated from equation (2 – 2) [43] where std is standard sample, u unknown or test sample, A absorption, I emission, and η refractive index.

$$\phi_u = \phi_{std} \left(\frac{A_{std}}{A_u}\right)\left(\frac{I_u}{I_{std}}\right)\left(\frac{\eta_u}{\eta_{std}}\right)^2 \qquad (2-2)$$

Transient Absorption

Time resolved transient absorption data were collected at North Carolina State University with an LP920 laser flash photolysis system (Edinburgh Instruments). The excitation source was the Vibrant LD 355 II Nd:YAG/OPO system (OPOTEK). Data acquisition was controlled by the LP900 software program (Edinburgh Instruments). Samples were prepared in spectrophotometric grade toluene or THF with an optical density of 0.3−0.5 at the excitation wavelength and were degassed with a minimum of three freeze-pump-thaw cycles. Kinetic traces were collected with a PMT (R928 Hamamatsu), and transient absorption spectra were collected with an iStar ICCD camera (Andor Technology).[44,45] The extinction coefficient of the dipyrrin triplet state was determined by energy transfer to perylene using equation (2 – 3). The dipyrrin triplet quantum yield was determined by relative actinometry using an aqueous $[Ru(bpy)_3]Cl_2$ standard according to equation (2 – 4). [44–46]

$$\varepsilon^{T}_{Donor} = \varepsilon^{T}_{Acceptor} \times \left(\frac{\Delta A_{Donor}}{\Delta A_{Acceptor}}\right) \times \Phi_{TTET} \qquad (2-3)$$

In equation (2 - 3), $\varepsilon^{T}_{Acceptor}$ is the triplet extinction coefficient of acceptor (from literature). ΔA_{Donor} is the maximum ΔA of the donor triplet at a given wavelength (from TA experiment). $\Delta A_{Acceptor}$ is the maximum ΔA of the acceptor triplet at wavelength where ε^{T} is reported (from TA experiment). Φ_{TTET} is the quantum yield of triplet-triplet energy transfer which it is determined from the Stern-Volmer constant.[43,44]

$$\Phi^{T}_{unk} = \Phi^{T}_{std}\left(\frac{\Delta A^{T}_{unk}}{\varepsilon^{T}_{unk}}\right)\left(\frac{\varepsilon^{T}_{std}}{\Delta A^{T}_{std}}\right)\left(\frac{\left(1-10^{Abs}\right)_{std}}{\left(1-10^{Abs}\right)_{unk}}\right) \qquad (2-4)$$

In equation (2 – 4), Φ^{T}_{unk} is the triplet state yield for unknown. Φ^{T}_{std} is the triplet state yield for standard (from literature). ΔA^{T}_{unk} is the maximum ΔA of unknown triplet. ε^{T}_{unk} is the unknown's triplet extinction coefficient at ΔA^{T}_{unk} wavelength. ΔA^{T}_{std} is the maximum ΔA of standard triplet. ε^{T}_{std} is the standard's triplet extinction coefficient at ΔA^{T}_{unk} wavelength (from literature). Abs is the ground state absorbance of standard or unknown at excitation wavelength.[43,44]

CHAPTER 3

RESULTS AND DISCUSSION

Synthesis and Characterization of ZnDPY and ZnIDPY

ZnDPY Complex

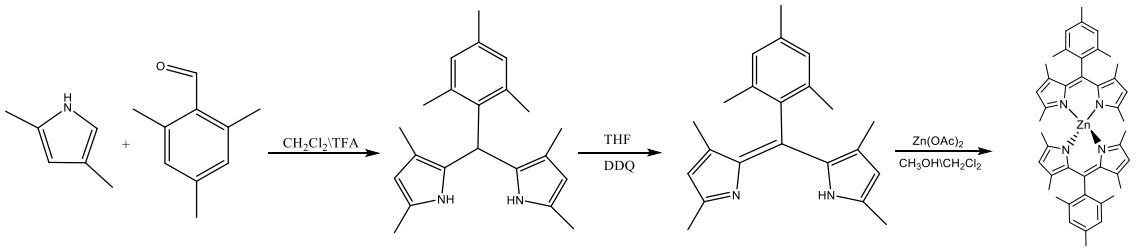

Figure 3.1. Synthetic scheme for producing ZnDPY

The first step in the synthesis of ZnDPY complex was 1, 3, 7, 9-tetramethyl-5-mesityldipyrromethane which was synthesized from 2,4-dimethylpyrrole and mesitaldehyde according to a published procedure.[9] The ^{1}H NMR spectrum matched the literature and the crude product was used for the next step without purification.

The product, 1, 3, 7, 9-tetramethyl-5-mesityldipyrromethane, was dehydrogenated by adding it to a solution of freshly distilled tetrahydrofuran (THF) and DDQ dissolved in THF under nitrogen with stirring for 1 h. After removing the solvent and washing the solution, the obtained product was 1, 3, 7, 9-tetramethyl-5-mesityldipyrromethene which was used for the final step without purification.[9]

The final procedure was adding the zinc(II) to the ligand. The product, ZnDPY complex, was obtained by adding a solution of zinc acetate dihydrate in methanol to a solution of 1, 3, 7, 9-tetramethyl-5-mesityldipyrromethene in dichloromethane under air.

The obtained solid was dissolved in the hexane/dichloromethane (7/3 v/v) mixture and passed through a short neutral alumina to separate the mixture into its pure components. After the orange-red portion was collected, the solvents were removed, and the solid was recrystallized from CH_2Cl_2/MeOH. The obtained ZnDPY complex was purified by sublimation.[9] ^1H and ^{13}C NMR were collected for the purified ZnDPY complex in $CDCl_3$. The results matched Thompson and co-workers results.[9] NMR positions and splitting are indicated in Table 3.1 below and shown in Figure 3.2. The protons of phenyl ring appeared at 6.92 ppm, and pyrrole protons are shown at 5.90 ppm. The protons of methyl groups showed from 1.29 to 2.34 ppm. Without further experiments the methyl protons cannot be assigned more specifically. The carbons of phenyl ring and pyrrole appeared from 119.63 to 155.99 ppm, and methyl groups' carbons showed from 14.91 to 21.30 ppm.

Table 3.1. Table of ^1H-NMR signals and their assignments for ZnDPY complex in $CDCl_3$

Position (ppm)	Splitting & Multiplicity	Assignment
6.92	Singlet, 4H	Phenyl ring
5.90	Singlet, 4H	Pyrrole
2.34	Singlet, 6H	CH_3 groups
2.10 – 2.02	Singlet, 24H	CH_3 groups
1.29	Singlet, 12H	CH_3 groups

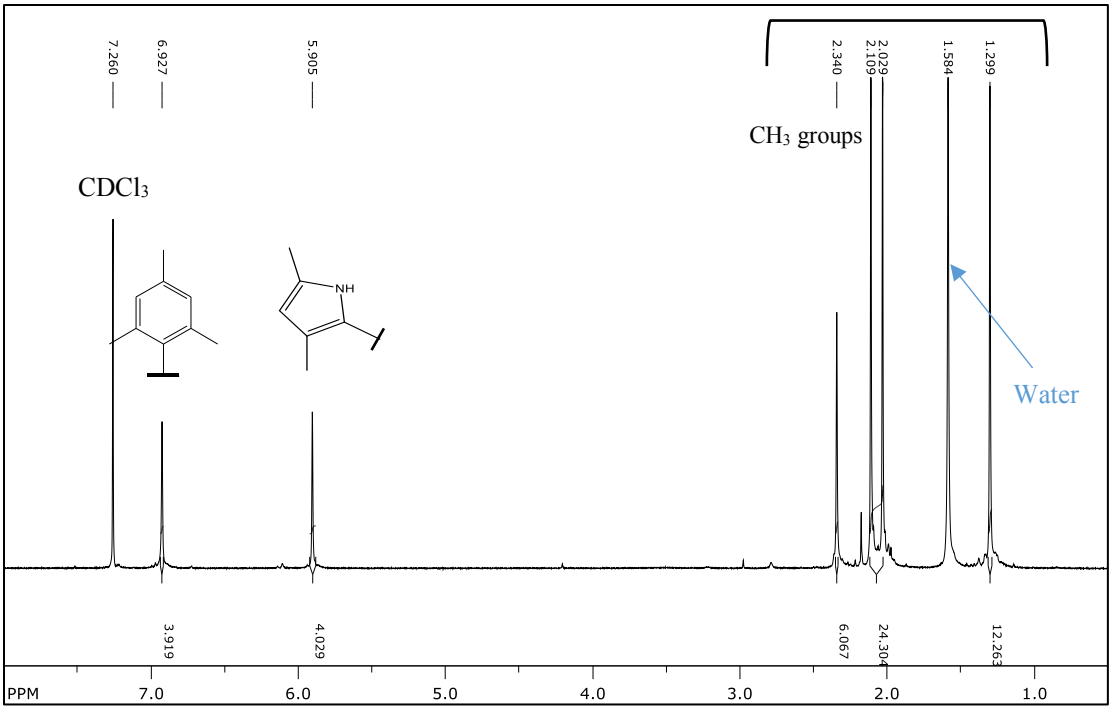

Figure 3.2. ^{1}H NMR of ZnDPY complex in $CDCl_3$

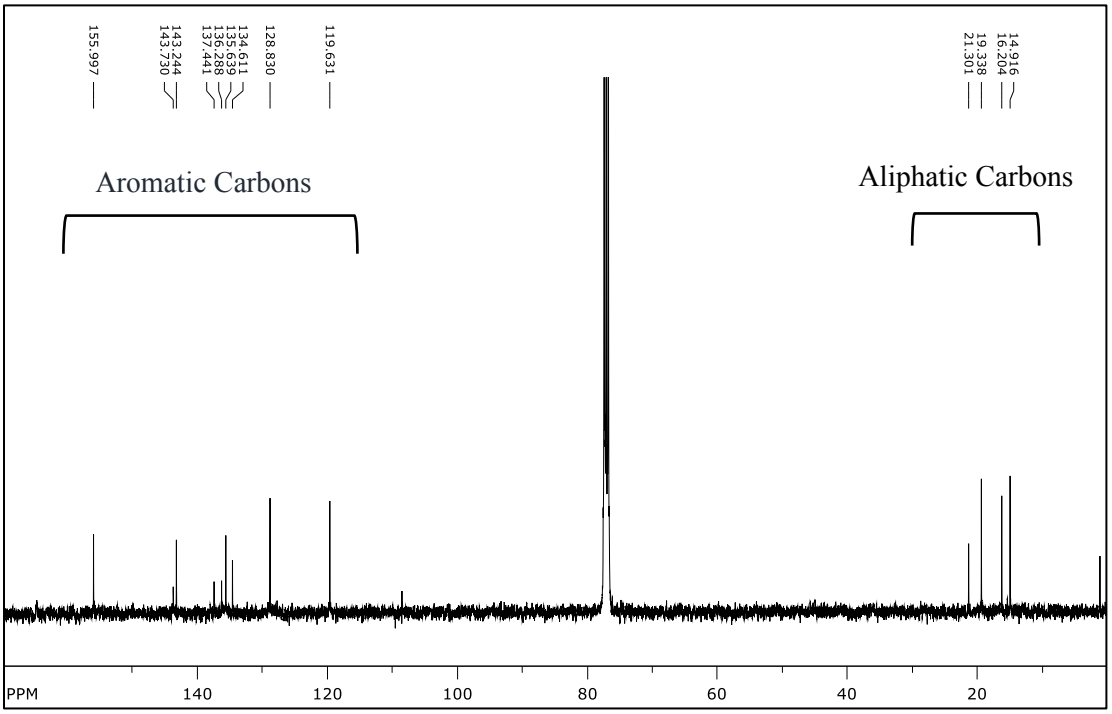

Figure 3.3. ^{13}C NMR of ZnDPY complex in $CDCl_3$

ZnIDPY Complex

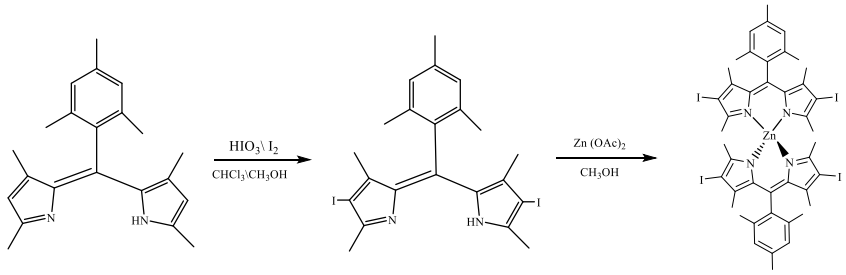

Figure 3.4. Synthetic scheme for producing ZnIDPY

2, 8- diiodo- 1, 3, 7, 9- tetramethyl-5- mesityldipyrromethene (IDPY) was produced by adding 1, 3, 7, 9-tetramethyl-5-mesityldipyrromethene to a 1:1 v/v solution of chloroform/methanol, iodine, and iodic acid according to a published procedure. The ^{1}H NMR of IDPY matched published values and the crude product was used without purification.[32]

The ZnIDPY complex was obtained by adding a solution of zinc acetate dihydrate and IDPY in methanol, and triethylamine was added to the mixture by following the published procedure.[39]The obtained solid was dissolved in dichloromethane and passed through a short neutral alumina to separate the mixture into its pure components. Then, the orange-red portion was collected, and the solvents were removed under reduced pressure. The ZnIDPY complex was further purified by recrystallization from CH_2Cl_2/MeOH.

^{1}H and ^{13}C NMR were collected for the purified ZnIDPY complex in $CDCl_3$. The ZnIDPY complex has not been previously synthesized, but the ^{1}H and ^{13}C NMR spectra bear a striking resemblance to the BODIPY complex of the IDPY ligand.[47] NMR positions and splitting are indicated in Table 3.2 below and shown in Figure 3.5. The

protons of phenyl ring appeared at 6.97 ppm. The pyrrole protons which appeared at 5.90 ppm in ZnDPY have completely disappeared in ZnIDPY, indicating the iodine substitution reaction was complete. The protons of methyl groups showed from 1.33 to 2.37 ppm. As with ZnDPY, the methyl protons cannot be more specifically assigned without further experiments. The carbons of phenyl ring and pyrrole appeared from 84.02 to 157.27 ppm, and methyl groups' carbons showed from 17.49 to 29.94 ppm.

Table 3. 2. Table of ^{1}H-NMR signals and their assignments for ZnIDPY complex in $CDCl_3$

Position (ppm)	Splitting & Multiplicity	Assignment
6.95	Singlet, 4H	Phenyl ring
2.36	Singlet, 6H	CH_3 groups
2.05-2.10	Singlet, 24H	CH_3 groups
1.31	Singlet, 12H	CH_3 groups

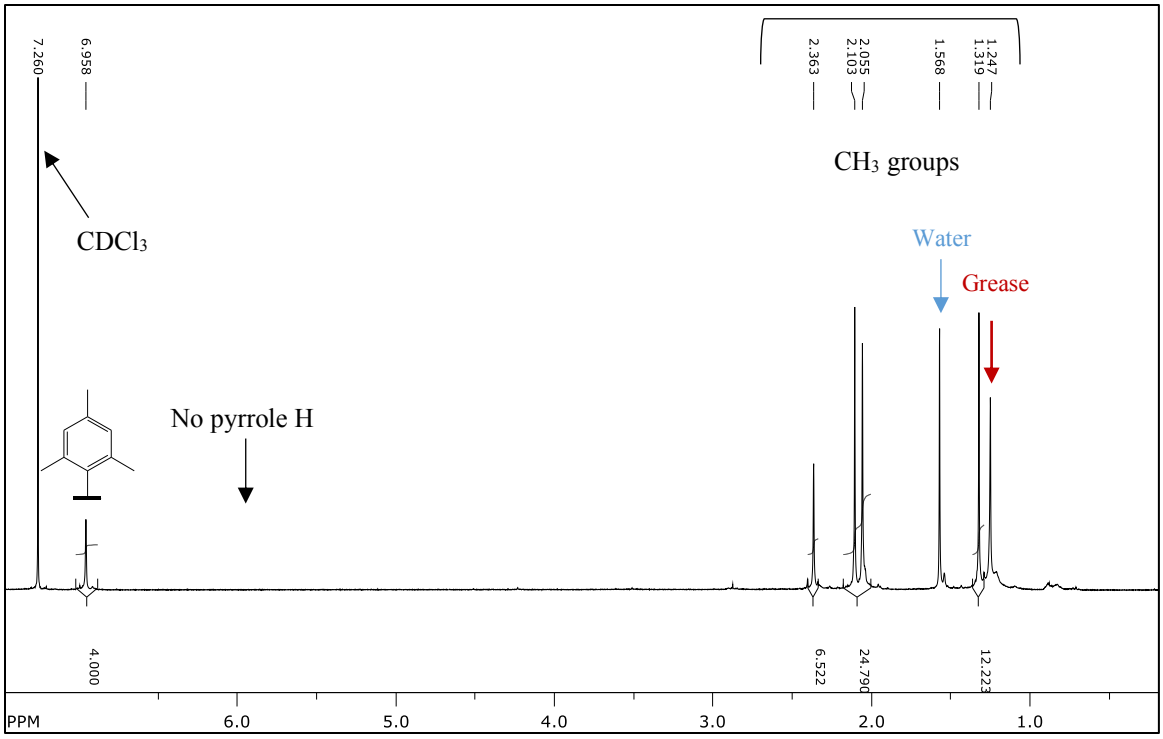

Figure 3.5. ^{1}H NMR of ZnIDPY complex in $CDCl_3$

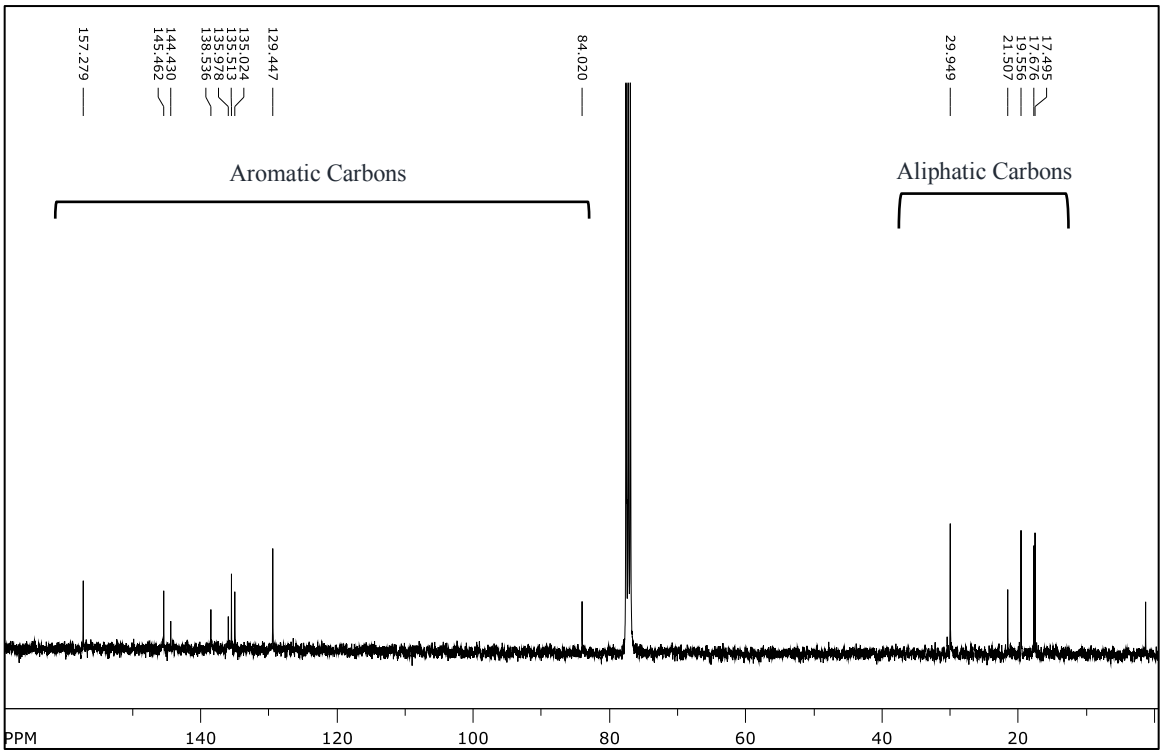

Figure 3.6. ^{13}C NMR of ZnIDPY complex in $CDCl_3$

Absorption Spectroscopy

The extinction coefficients of both ZnDPY and ZnIDPY complexes in toluene were measured according to Beer's Law.[40] The absorbance versus specific wavelength is to determine the absorption at maximum wavelength λ_{max}. The line of the absorbance versus concentration should go through the point 0.0 at 0.00 M concentration. The slope of the line is the extinction coefficient, ε. The UV-vis spectra of ZnDPY and ZnIDPY in toluene are shown in Figures 3.7 and 3.9. The absorption spectra of both complexes are dominated by a single, intense transition. The absorption maxima for ZnDPY and ZnIDPY are 490 nm and 515 nm, respectively. The absorption peaks of the two complexes are due to ligand localized $\pi \rightarrow \pi^*$ transitions. The results showed that the absorption of ZnIDPY complex shifts to lower energy due to inserting the iodine. The iodine is electron withdrawing and causes the energy gap between the HOMO and LUMO orbitals to change by removing electron density from π-system, so π-bonding becomes weak, and the energy difference between the HOMO and LUMO orbitals decreases. The straight line indicates a plot of the absorbances versus different concentrations where the slope gives the value of extinction coefficient as shown in Figures 3.8 and 3.10. The ZnDIPY complex has a higher value of extinction coefficient and intensity than ZnDPY complex as illustrated in Figure 3.11. Table 3.3 summarizes the results of three replicated trials of extinction coefficient of each complex in toluene.

Table 3. 3. Absorption properties of ZnDPY and ZnIDPY in toluene

	λ_{max}	ε (λ_{max})	Average ε
ZnDPY	490 nm	122,000 $M^{-1}cm^{-1}$ 123,000 $M^{-1}cm^{-1}$ 101,000 $M^{-1}cm^{-1}$	116,000 $M^{-1}cm^{-1} \pm$ 12,000
ZnIDPY	515 nm	176,000 $M^{-1}cm^{-1}$ 154,000 $M^{-1}cm^{-1}$ 154,000 $M^{-1}cm^{-1}$	161,000 $M^{-1}cm^{-1} \pm$ 12,000

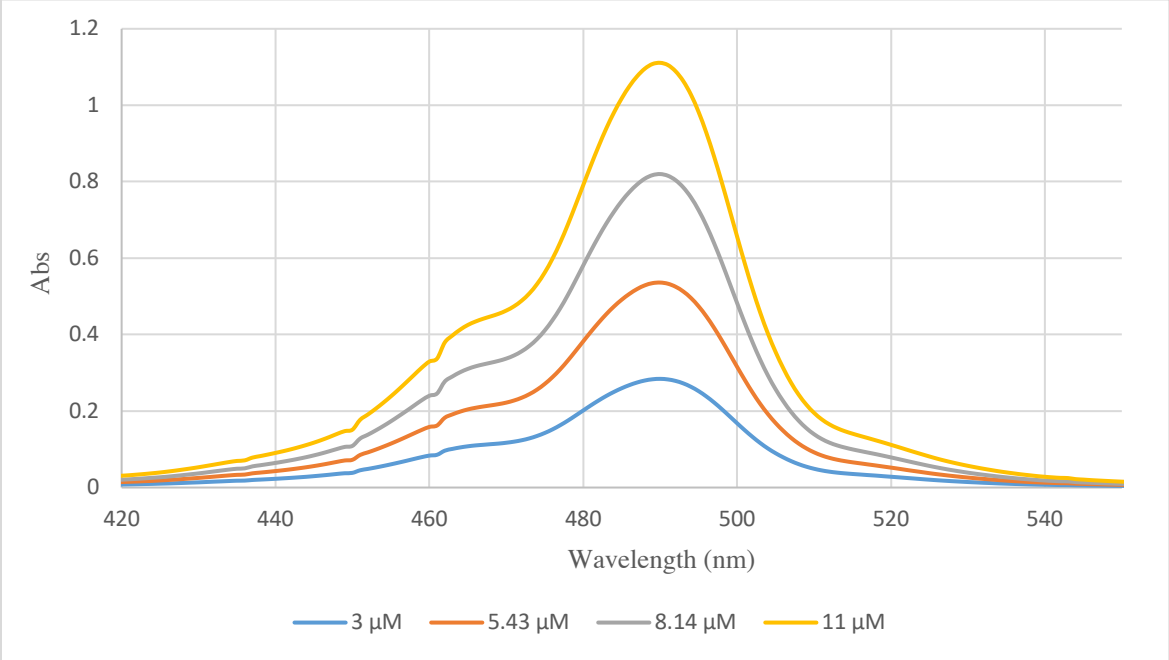

Figure 3.7. Absorption spectra of ZnDPY complex in toluene for different concentrations

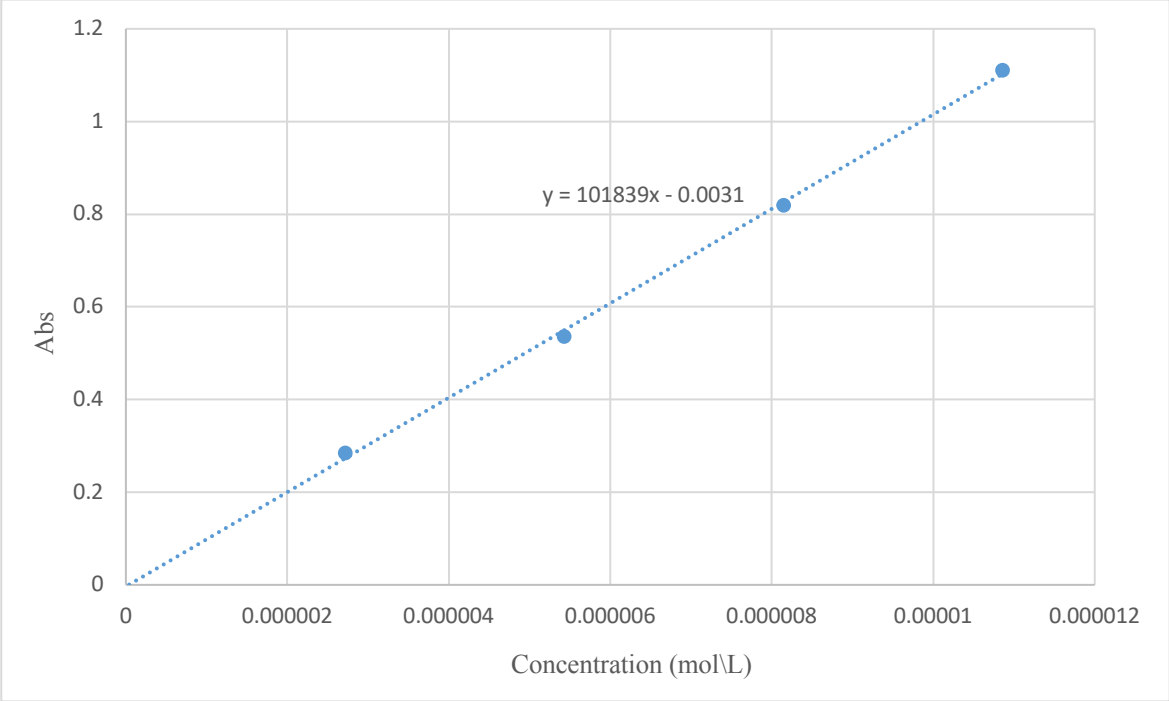

Figure 3.8. Example of a Beer's Law plot for ZnDPY in toluene

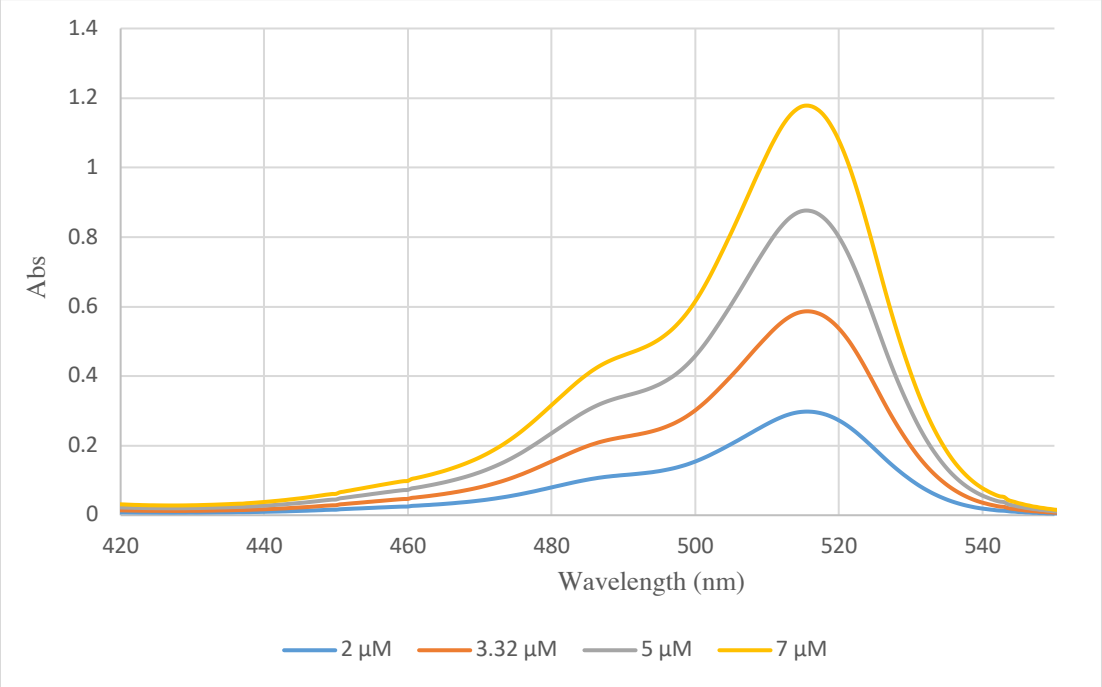

Figure 3.9. Absorption spectra of ZnIDPY complex in toluene for different concentrations

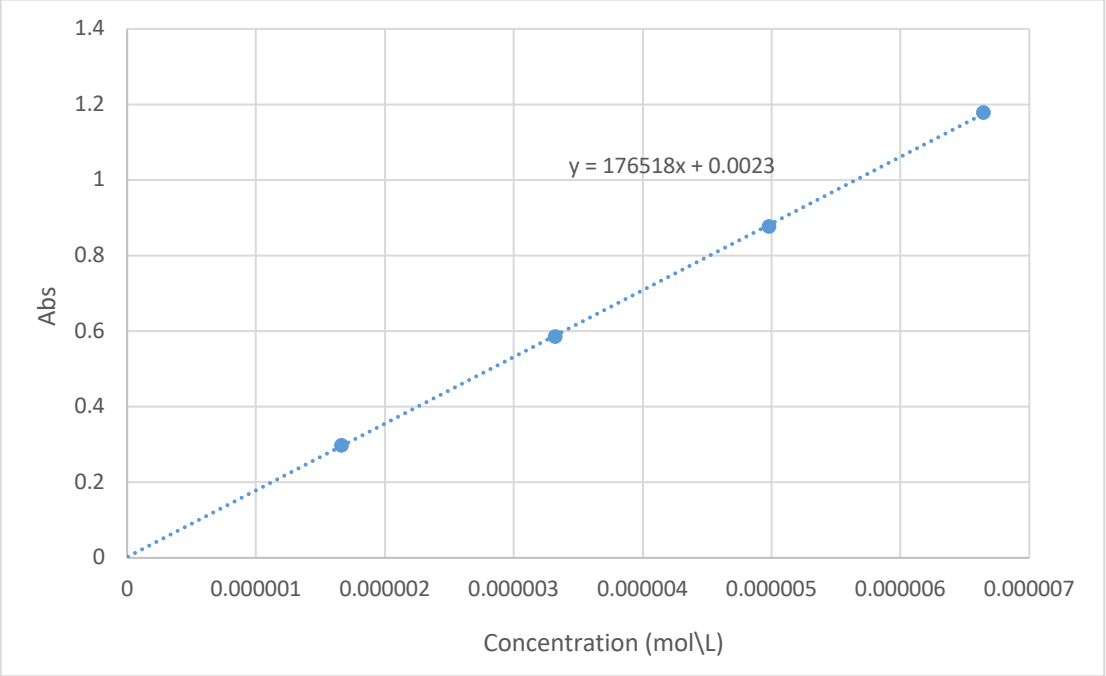

Figure 3.10. Example of a Beer's Law plot for ZnIDPY in toluene

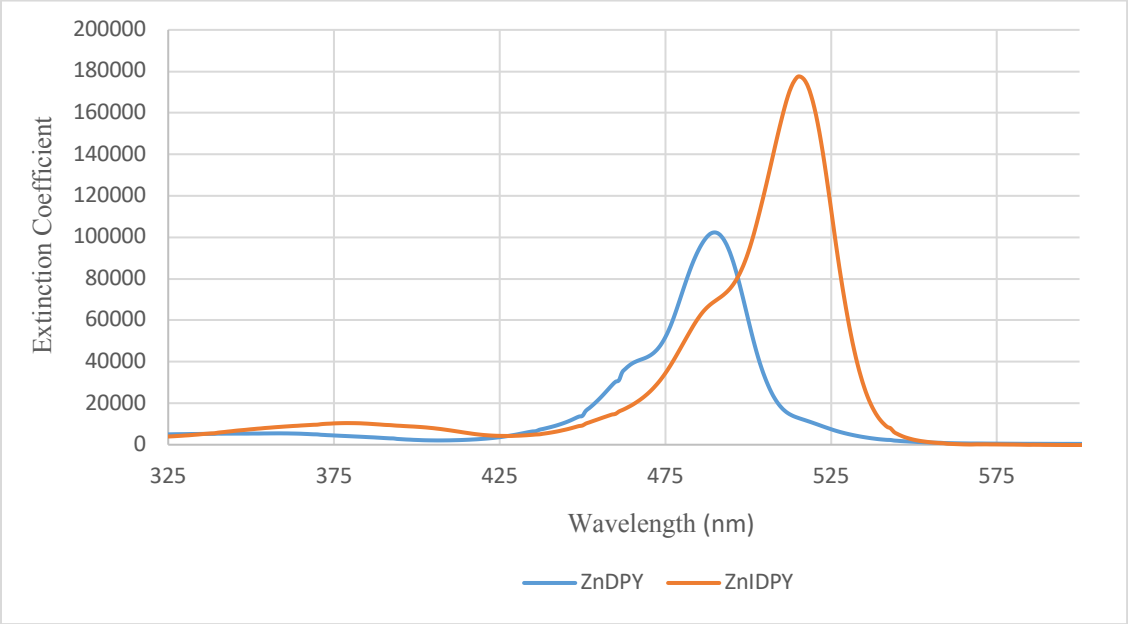

Figure 3.11. The extinction coefficients of the two ZnDPY and ZnIDPY in toluene

Emission Spectroscopy

The emission spectra of ZnDPY and ZnIDPY in toluene and THF are shown in Figures 3.12 - 3.17. The complexes were found to display photoluminescence with emission maxima ranging from 509 nm in ZnDPY to 532 nm in ZnIDPY. The emission in both complexes is fluorescence emission from $S_1 \rightarrow S_0$ under air. The photoluminescence quantum yield of the two ZnDPY and ZnIDPY complexes were measured in both toluene and THF solvents. $[Ru(bpy)_3]Cl_2$ in aerated water ($\Phi = 0.04$)[41] was used as the standard because it absorbs at the same excitation wavelength as the two complexes and has a similar emission wavelength and intensity as the dipyrrin complexes. The fluorescence emissions of the two complexes are strongly solvent-dependent because of the presence of the CS. The results showed in nonpolar solvent (toluene) higher photoluminescence quantum yield than in polar solvent (THF). The photoluminescence quantum yield in polar solvent is low because the CS state is stabilized and becomes lower in energy than the fluorescent singlet excited state (S_1). The ZnIDPY complex showed a lower quantum yield than ZnDPY complex due to having a heavy atom, so we hypothesize that will enhance the ISC between the CS and T_1 states as it happened between the S_1 and T_1 states in boron dipyrrin complexes. Table 3.4 exhibits the values of three replicated trials of photoluminescence quantum yield of each complex in toluene and THF.

Table 3. 4. The photoluminescence quantum yield values of the two ZnDPY and ZnIDPY complexes in toluene and THF

	Toluene ϕ_{PL}	Average ϕ_{PL}	THF ϕ_{PL}	Average ϕ_{PL}
ZnDPY	0.128 0.124 0.123	0.125 ± 0.0025	0.04 0.032 0.048	0.04 ± 0.0077
ZnDIPY	0.019 0.018 0.018	0.02 ± 0.0001	0.0014 0.0010 0.0011	0.001 ± 0.00022

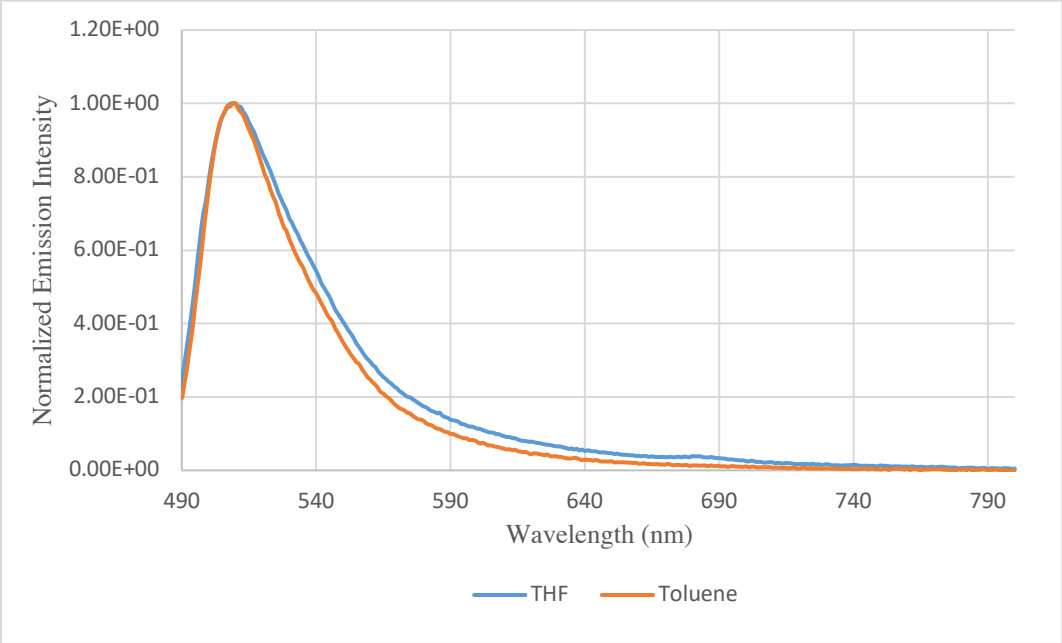

Figure 3.12. Normalized emission of ZnDPY in toluene and THF

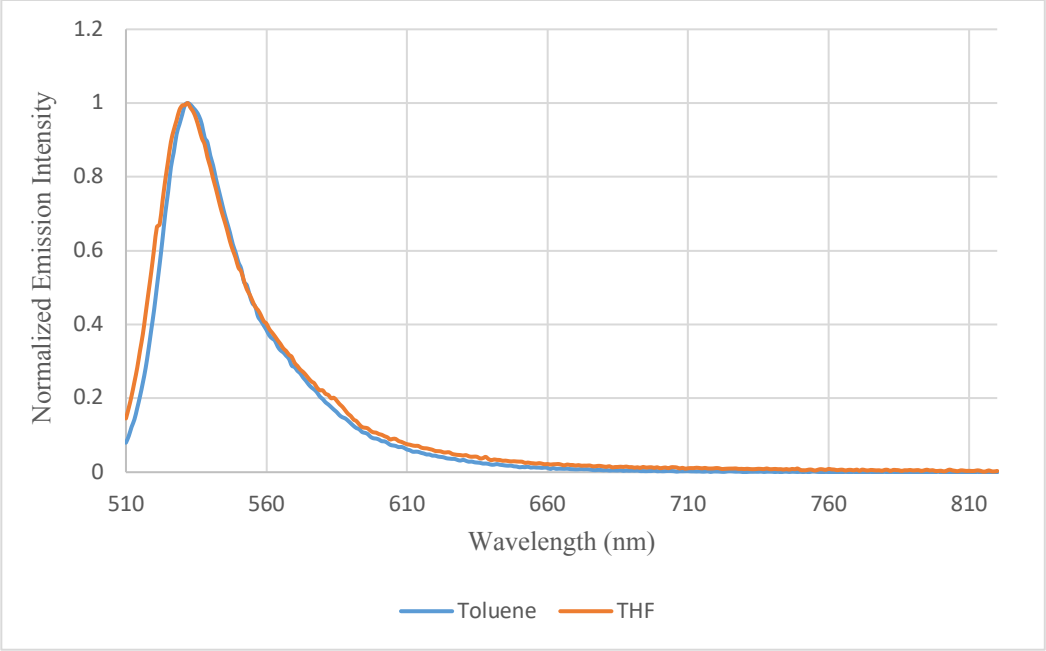

Figure 3.13. Normalized emission of ZnIDPY in toluene and THF

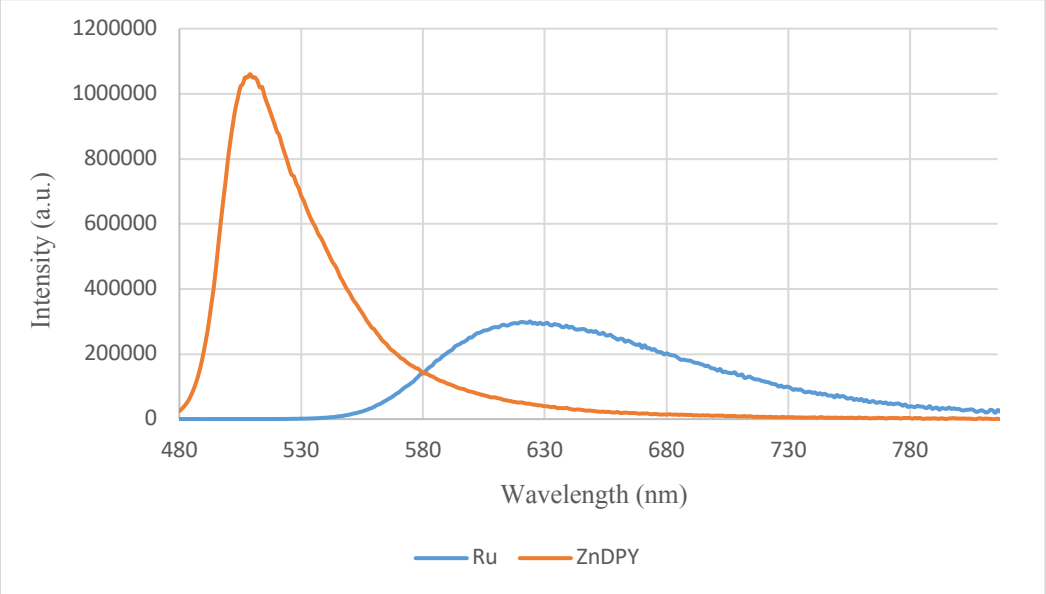

Figure 3.14. Emission spectra of ZnDPY in toluene and standard $[Ru(bpy)_3]Cl_2$

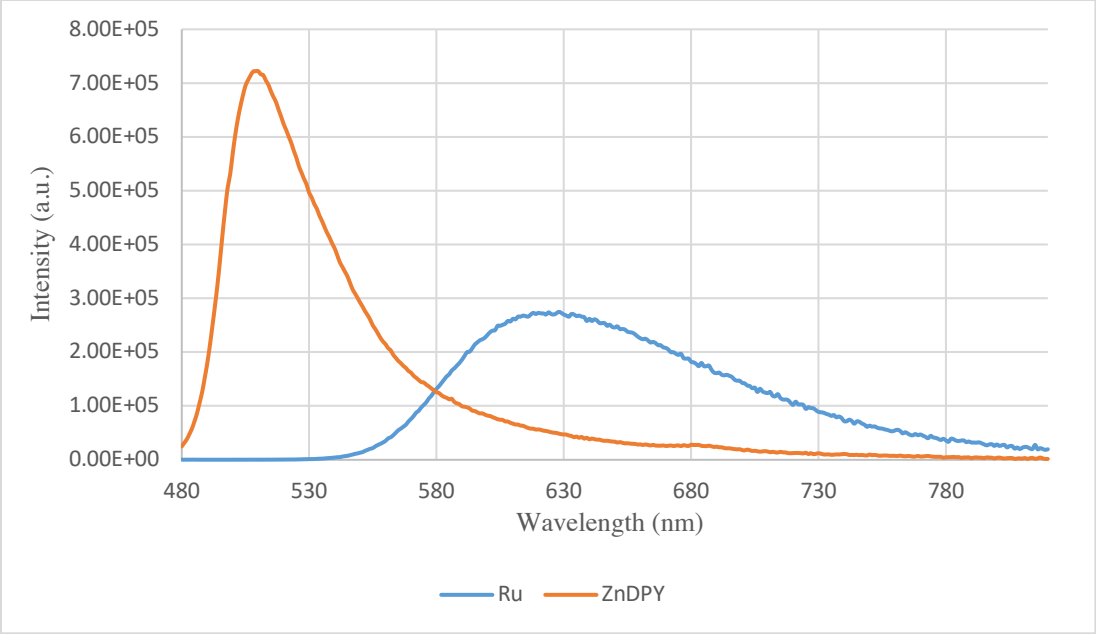

Figure 3.15. Emission spectra of ZnDPY in THF and standard $[Ru(bpy)_3]Cl_2$

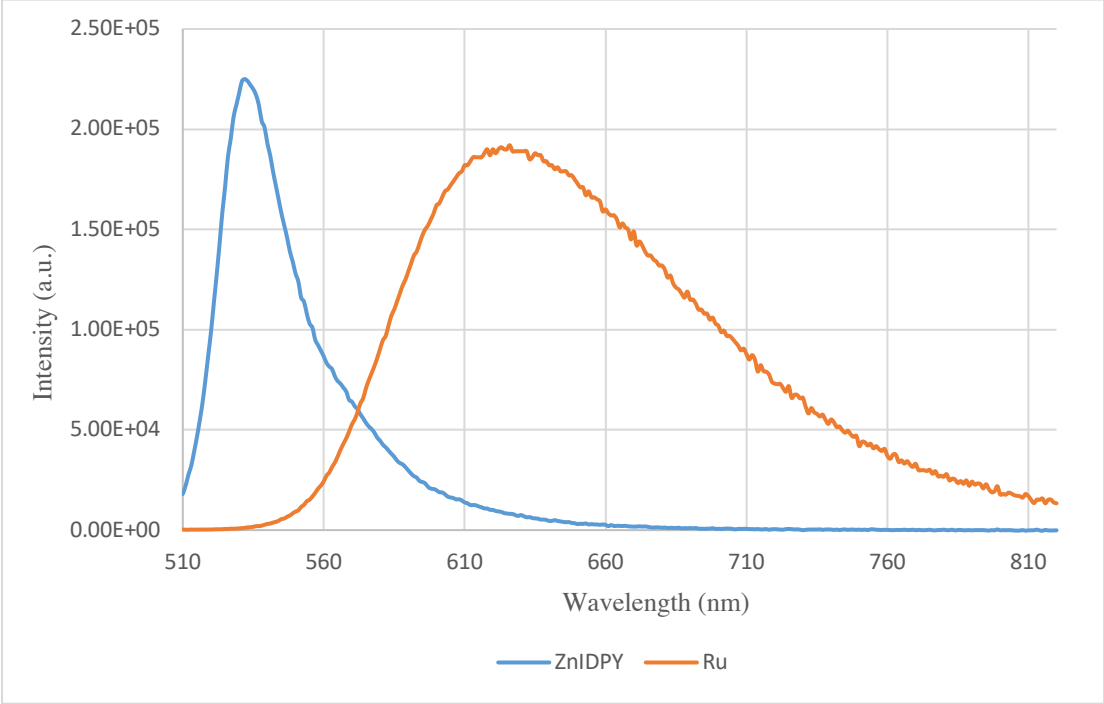

Figure 3.16. Emission spectra of ZnIDPY in toluene and standard $[Ru(bpy)_3]Cl_2$

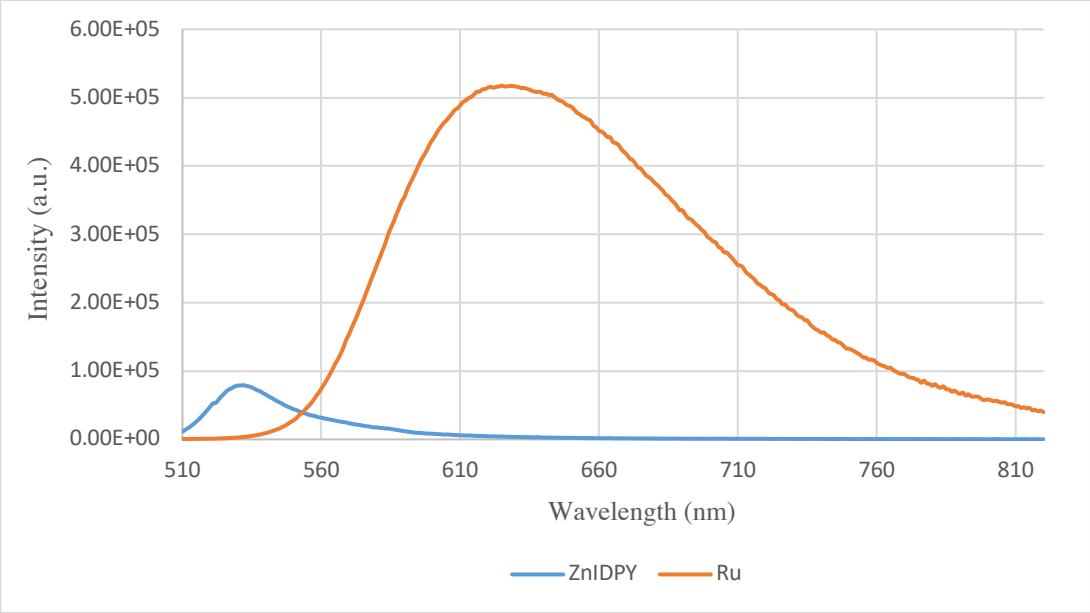

Figure 3.17. Emission spectra of ZnIDPY in THF and standard $[Ru(bpy)_3]Cl_2$

Transient Absorption

Figure 3.18 below shows the nanosecond transient absorption difference spectra of ZnDPY and ZnIDPY in deaerated THF solution collected 50 μs after excitation by laser at 480 nm for ZnDPY and at 500 nm for ZnIDPY to capture their triplet excited state at room temperature. The transient absorption studies which are shown in Figure 3.18 confirm the formation of a long-lived excited state in deaerated room temperature THF solution whose spectral shape is similar to the triplet state spectra reported in other Zn(II) dipyrrin complexes.[9] The quantum yield of triplet state formation for the two complexes is determined in two steps. First, the extinction coefficient of the triplet state is determined by energy transfer to a known triplet acceptor (perylene). Second, the quantum yield of triplet state formation is determined relative to a standard ($[Ru(bpy)_3]Cl_2$) with a known triplet quantum yield and extinction coefficient.[44–46]

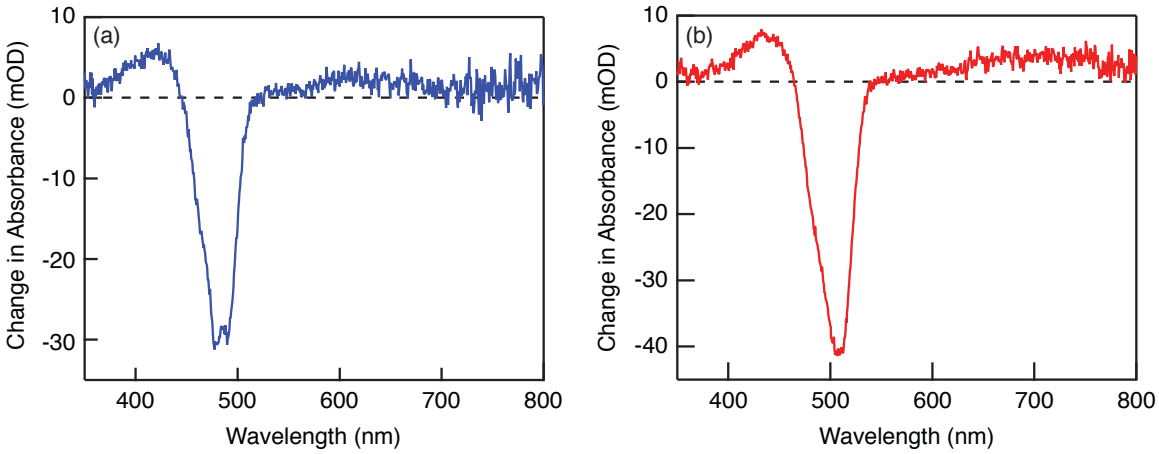

Figure 3.18. Nanosecond transient absorption difference spectrum of (a) ZnDPY and (b) ZnIDPY in deaerated THF solution collected 50 μs after laser excitation

The extinction coefficients of the triplet state for both ZnDPY and ZnIDPY complexes were measured by energy transfer to a compound with a known triplet extinction coefficient, perylene (ε_{490} = 14300 $M^{-1}cm^{-1}$).[43] Accurate determination of triplet extinction coefficient by the energy transfer method requires an acceptor with a known triplet extinction coefficient and all quenching of the donor must occur by energy transfer to the acceptor. Also, there must be selective excitation for the donor, and all the acceptor triplets should form through energy transfer from donor. The reaction below illustrates the general idea of transient absorption. After the excitation by laser, the excited state of the donor, D^*, (ZnDPY or ZnIDPY) transfers energy to the acceptor, A, (perylene) to form the triplet acceptor ($^3A^*$). The intensity of the transient absorption signal for the donor excited state and the acceptor excited state are compared to determine the donor's triplet extinction coefficient. Table 3.5 exhibits the values of triplet state extinction coefficient. [44,45]

$$D + A \xrightarrow{h\nu} D^* + A \xrightarrow{TTET} D + {}^3A^* \qquad (3-1)$$

Table 3. 5. Triplet state extinction coefficient values of ZnDPY and ZnIDPY donor in toluene and THF

	Solvents	λ_{ex}	λ_{probe}	ε_{donor}
ZnDPY	Toluene	490 nm	600 nm	3007 $M^{-1}cm^{-1}$
ZnDPY	THF	490 nm	600 nm	3106 $M^{-1}cm^{-1}$
ZnIDPY	THF	510 nm	440 nm	18296 $M^{-1}cm^{-1}$
ZnIDPY	THF	510 nm	700 nm	6426 $M^{-1}cm^{-1}$

After the triplet extinction coefficient of the donor was measured by using energy transfer method, the quantum yield of the triplet state formation can be determined by relative actinometry. The triplet extinction coefficient of both species and the triplet state yield for the standard ($[Ru(bpy)_3]Cl_2$) should be known. The ground state depletion needs to be relatively small, and the ground state absorbance of the standard and unknown solutions should match at the excitation wavelength.[44,45] Tables 3.6 and 3.7 show the results of the triplet state quantum yield of ZnDPY in THF and toluene from a single measurement and the average of two measurements at two probe wavelengths for ZnIDPY in THF. Comparing the triplet yield of ZnDPY in toluene and THF, the quantum yield increases in the more polar THF in agreement with the initial hypothesis. When comparing the triplet quantum yield of ZnDPY and ZnIDPY in THF, it is clear that the presence of iodine does not increase the formation of triplet state as hypothesized.

Table 3. 6. Triplet state quantum yield values of ZnDPY in toluene and THF

	Solvents	λ_{ex}	Φ_{unk}^{T}
ZnDPY	Toluene	490 nm	0.209
ZnDPY	THF	490 nm	0.411

Table 3. 7. Triplet state quantum yield values of ZnDPY and ZnIDPY in THF

	Solvents	λ_{ex}	Φ_{unk}^{T}
ZnDPY	THF	490 nm	0.411
ZnIDPY	THF	510 nm	0.325 ± 0.012

CHAPTER 4

CONCLUSION

The goals of this research were to synthesize and characterize the two ZnDPY and ZnIDPY photosensitizers, to study their photophysical properties, and to perform qualitative identification of triplet formation for them and quantify their yield of triplet state formation.

The presence of a photosensitizer is one of the requirements for photocatalytic carbon dioxide reduction. Complexes of the dipyrrin ligand are known to have the criteria to be good photosensitizers. Zinc(II) dipyrrins complexes form a long-lived triplet state which has been spectroscopically observed by the Thompson group.[9] Forming a long-lived triplet state increases their ability to be effective photosensitizers. Thus, the ZnDPY, which had been synthesized by Thompson and co-workers, has also been synthesized in this research to study its properties and to measure the quantum yield of the triplet state. The new zinc(II) iodine dipyrrin complex (ZnIDPY) was synthesized because we hypothesized that inserting the iodine would enhance the ISC between the CS and T_1 states as it happened between the S_1 and T_1 states in boron dipyrrin complexes.

After the two ZnDPY and ZnIDPY complexes had been synthesized and purified, they were characterized by using NMR, mass spectroscopy, and elemental analysis. The photophysical properties of the two complexes were obtained, particularly extinction coefficient and fluorescence quantum yield, in both polar and non-polar solvents. The decreased photoluminescence quantum yield in a polar solvent is because the CS state is stabilized and becomes lower in energy than the fluorescent singlet excited state (S_1). The

ZnIDPY complex has shown a lower fluorescence quantum yield than the ZnDPY complex due to having a heavy atom, supporting the hypothesis which predicted the iodine would enhance the ISC between the CS and T_1 states. The formation of a long-lived excited state in deaerated room temperature solution has been shown for both ZnDPY and ZnIDPY compounds by using nanosecond transient absorption. Through transient absorption spectroscopy, the triplet state quantum yield of both complexes was also measured to determine the effect of solvent polarity and heavy atoms on the triplet state formation. The results showed that in ZnDPY, increasing the solvent polarity does increase the quantum yield of the triplet state, in agreement with the initial hypothesis. Comparing the triplet state quantum yields of ZnDPY and ZnIDPY gives an unexpected result. The triplet quantum yield for ZnIDPY is lower than ZnDPY, disproving the hypothesis that the presence of iodine atoms would enhance the formation of triplet excited states. Further study is needed to verify and investigate this result.

Future Aims

After the zinc(II) dipyrrin complexes are synthesized, their physical properties are studied, and the formation of their triplet state is proved, the electrochemical potentials will be measured in polar and nonpolar solvents to identify the excited state redox potentials and see if the Zn sensitizers are energetically capable of reducing the catalyst. In addition, Zn(II) sensitizer will be mixed with catalyst and electron donor to perform photocatalysis to convert carbon dioxide into fuel.

REFERENCES

(1) Dudley, B. BP Statistical Review of World Energy 2016. https://www.bp.com/content/dam/bp/pdf/energy-economics/statistical-review-2016/bp-statistical-review-of-world-energy-2016-full-report.pdf (accessed May 3, 2018).

(2) Benson, E. E.; Kubiak, C. P.; Sathrum, A. J.; Smieja, J. M. Electrocatalytic and Homogeneous Approaches to Conversion of CO_2 to Liquid Fuels. *Chem. Soc. Rev.* **2009**, *38*, 89–99.

(3) Lingampalli, S. R.; Ayyub, M. M.; Rao, C. N. R. Recent Progress in the Photocatalytic Reduction of Carbon Dioxide. *ACS Omega.* **2017**, *2*, 2740–2748.

(4) Leen, V.; Miscoria, D.; Yin, S.; Filarowski, A.; Molisho Ngongo, J.; Van der Auweraer, M.; Boens, N.; Dehaen, W. 1,7-Disubstituted Boron Dipyrromethene (BODIPY) Dyes: Synthesis and Spectroscopic Properties. *J. Org. Chem.* **2011**, *76*, 8168–8176.

(5) Bañuelos, J.; Arroyo-Córdoba, I. J.; Valois-Escamilla, I.; Alvarez-Hernández, A.; Peña-Cabrera, E.; Hu, R.; Zhong Tang, B.; Esnal, I.; Martínez, V.; López Arbeloa, I. Modulation Of The Photophysical Properties Of BODIPY Dyes By Substitution At Their Meso Position. *RSC Advances.* **2011**, *1*, 677.

(6) Ziessel, R.; Ulrich, G.; Haefele, A.; Harriman, A. An Artificial Light-Harvesting Array Constructed from Multiple Bodipy Dyes. *J. Am. Chem. Soc.* **2013**, *135*, 11330–11344.

(7) Lincoln, R.; Greene, L. E.; Krumova, K.; Ding, Z.; Cosa, G. Electronic Excited State Redox Properties for BODIPY Dyes Predicted from Hammett Constants:

Estimating the Driving Force of Photoinduced Electron Transfer. *J. Phys. Chem. A* **2014**, *118*, 10622–10630.

(8) Kusaka, S.; Sakamoto, R.; Kitagawa, Y.; Okumura, M.; Nishihara, H. An Extremely Bright Heteroleptic Bis(Dipyrrinato)Zinc(II) Complex. *Chem. Asian. J* **2012**, *7*, 907–910.

(9) Trinh, C.; Kirlikovali, K.; Das, S.; Ener, M. E.; Gray, H. B.; Djurovich, P.; Bradforth, S. E.; Thompson, M. E. Symmetry-Breaking Charge Transfer of Visible Light Absorbing Systems: Zinc Dipyrrins. *J. Phys. Chem. C* **2014**, *118*, 21834–21845.

(10) Wood, T. E.; Thompson, A. Advances in the Chemistry of Dipyrrins and Their Complexes. *Chem. Rev* **2007**, *107*, 1831–1861.

(11) Tsuchiya, M.; Sakamoto, R.; Shimada, M.; Yamanoi, Y.; Hattori, Y.; Sugimoto, K.; Nishibori, E.; Nishihara, H. Bis(Dipyrrinato)Zinc(II) Complexes: Emission in the Solid State. *Inorg. Chem.* **2016**, *55*, 5732–5734.

(12) Scharf, A. B. First-Row Transition Metal Complexes of Dipyrrinato Ligands: Synthesis and Characterization. Doctoral dissertation, Harvard University, 2013.

(13) Bonin, J.; Robert, M.; Routier, M. Selective and Efficient Photocatalytic CO_2 Reduction to CO Using Visible Light and an Iron-Based Homogeneous Catalyst. *J. Am. Chem. Soc.* **2014**, *136*, 16768–16771.

(14) Fontaine, F.-G.; Courtemanche, M.-A.; Légaré, M.-A. Transition-Metal-Free Catalytic Reduction of Carbon Dioxide. *Chem. – Eur. J* **2014**, *20*, 2990–2996.

(15) Takeda, H.; Ohashi, K.; Sekine, A.; Ishitani, O. Photocatalytic CO_2 Reduction Using Cu(I) Photosensitizers with a Fe(II) Catalyst. *J. Am. Chem. Soc.* **2016**, *138*, 4354–4357.

(16) Takeda, H.; Cometto, C.; Ishitani, O.; Robert, M. Electrons, Photons, Protons and Earth-Abundant Metal Complexes for Molecular Catalysis of CO_2 Reduction. *ACS Catalysis.* **2017**, *7*, 70–88.

(17) Agarwal, J.; Shaw, T. W.; Schaefer, H. F.; Bocarsly, A. B. Design of a Catalytic Active Site for Electrochemical CO_2 Reduction with Mn(I)-Tricarbonyl Species. *Inorg. Chem.* **2015**, *54*, 5285–5294.

(18) Riplinger, C.; Sampson, M. D.; Ritzmann, A. M.; Kubiak, C. P.; Carter, E. A. Mechanistic Contrasts between Manganese and Rhenium Bipyridine Electrocatalysts for the Reduction of Carbon Dioxide. *J. Am. Chem. Soc.* **2014**, *136*, 16285–16298.

(19) Rawat, K. S.; Mahata, A.; Choudhuri, I.; Pathak, B. N-Heterocylic Carbene-Based Mn Electrocatalyst for Two-Electron CO_2 Reduction over Proton Reduction. *J. Phys. Chem. C* **2016**, *120*, 8821–8831.

(20) Costentin, C.; Drouet, S.; Robert, M.; Saveant, J.-M. A Local Proton Source Enhances CO2 Electroreduction to CO by a Molecular Fe Catalyst. *Science* **2012**, *338*, 90–94.

(21) Alsabeh, P. G.; Rosas-Hernández, A.; Barsch, E.; Junge, H.; Ludwig, R.; Beller, M. Iron-Catalyzed Photoreduction of Carbon Dioxide to Synthesis Gas. *Catal. Sci. Technol.* **2016**, *6*, 3623–3630.

(22) Lian, S.; Kodaimati, M. S.; Dolzhnikov, D. S.; Calzada, R.; Weiss, E. A. Powering a CO_2 Reduction Catalyst with Visible Light through Multiple Sub-Picosecond Electron Transfers from a Quantum Dot. *J. Am. Chem. Soc.* **2017**, *139*, 8931–8938.

(23) Chan, S. L.-F.; Lam, T. L.; Yang, C.; Yan, S.-C.; Cheng, N. M. A Robust and Efficient Cobalt Molecular Catalyst for CO_2 Reduction. *Chem. Commun.* **2015**, *51*, 7799–7801.

(24) Mase, K.; Aoi, S.; Ohkubo, K.; Fukuzumi, S. Catalytic Reduction of Proton, Oxygen and Carbon Dioxide with Cobalt Macrocyclic Complexes. *J. Porphyr. Phthalocyanines.* **2016**, *20*, 935–949.

(25) Roy, S.; Sharma, B.; Pécaut, J.; Simon, P.; Fontecave, M.; Tran, P. D.; Derat, E.; Artero, V. Molecular Cobalt Complexes with Pendant Amines for Selective Electrocatalytic Reduction of Carbon Dioxide to Formic Acid. *J. Am. Chem. Soc.* **2017**, *139*, 3685–3696.

(26) Mejeritskaia, E.; Luo, F.; Kelly, C. A.; Koch, B.; Gundlach, E. M.; Blinn, E. L. The Reduction of Carbon Dioxide Employing 1,4,7, Lo-Tetramethyl- 1,4,7,10 Tetraazacyclododecane Nickel(I1) as a Electron Relay Catalyst. *Inorg. Chim. Acta.* **1996**, 5.

(27) Breedlove, B. K.; Ferrence, G. M.; Washington, J.; Kubiak, C. P. A Photoelectrochemical Approach to Splitting Carbon Dioxide for a Manned Mission to Mars. *Materials & Design* **2001**, *22*, 577–584.

(28) Rakowski Dubois, M.; Dubois, D. L. Development of Molecular Electrocatalysts for CO_2 Reduction and H_2 Production/Oxidation. *Acc. Chem. Res.* **2009**, *42*, 1974–1982.

(29) Fogg, P. G. T. *Carbon Dioxide in Non–Aqueous Solvents At Pressures Less Than 200 KPA*; Elsevier, 1992.

(30) Elbjeirami, O.; Rawashdeh-Omary, M. A.; Omary, M. A. Phosphorescence Sensitization via Heavy-Atom Effects in D10 Complexes. *Res. Chem. Intermed.* **2011**, *37*, 691–703.

(31) Palmer, J. H.; Durrell, A. C.; Gross, Z.; Winkler, J. R.; Gray, H. B. Near-IR Phosphorescence of Iridium(III) Corroles at Ambient Temperature. *J. Am. Chem. Soc.* **2010**, *132*, 9230–9231.

(32) Sakamoto, R.; Iwashima, T.; Kögel, J. F.; Kusaka, S.; Tsuchiya, M.; Kitagawa, Y.; Nishihara, H. Dissymmetric Bis(Dipyrrinato)Zinc(II) Complexes: Rich Variety and Bright Red to Near-Infrared Luminescence with a Large Pseudo-Stokes Shift. *J. Am. Chem. Soc.* **2016**, *138*, 5666–5677.

(33) Kee, H. L.; Kirmaier, C.; Yu, L.; Thamyongkit, P.; Youngblood, W. J.; Calder, M. E.; Ramos, L.; Noll, B. C.; Bocian, D. F.; Scheidt, W. R.; et al. Structural Control of the Photodynamics of Boron−Dipyrrin Complexes. *J. Phys. Chem.B* **2005**, *109*, 20433–20443.

(34) Satake, A.; Kobuke, Y. Artificial Photosynthetic Systems: Assemblies of Slipped Cofacial Porphyrins and Phthalocyanines Showing Strong Electronic Coupling. *Org. Biomol. Chem.* **2007**, *5*, 1679.

(35) Sazanovich, I. V.; Kirmaier, C.; Hindin, E.; Yu, L.; Bocian, D. F.; Lindsey, J. S.; Holten, D. Structural Control of the Excited-State Dynamics of Bis(Dipyrrinato)Zinc Complexes: Self-Assembling Chromophores for Light-Harvesting Architectures. *J. Am. Chem. Soc.* **2004**, *126*, 2664–2665.

(36) Wu, W.; Guo, H.; Wu, W.; Ji, S.; Zhao, J. Organic Triplet Sensitizer Library Derived from a Single Chromophore (BODIPY) with Long-Lived Triplet Excited State for Triplet–Triplet Annihilation Based Upconversion. *J. Org. Chem.* **2011**, *76*, 7056–7064.

(37) Sabatini, R. P.; Lindley, B.; McCormick, T. M.; Lazarides, T.; Brennessel, W. W.; McCamant, D. W.; Eisenberg, R. Efficient Bimolecular Mechanism of Photochemical Hydrogen Production Using Halogenated Boron-Dipyrromethene (Bodipy) Dyes and a Bis(Dimethylglyoxime) Cobalt(III) Complex. *J. Phys. Chem. B* **2016**, *120*, 527–534.

(38) Guseva, G. B.; Antina, E. V.; Beresin, M. B.; V'yugin, A. I.; Nuraneeva, E. N. Preparation, Spectral and Thermal Properties of Co(II), Ni(II), Cu(II), Zn(II), and Cd(II) Complexes with Iodosubstituted 2,2′-Dipyrrolylmethene. *Russ. J. Gen. Chem.* **2013**, *83*, 1571–1579.

(39) Dudina, N. A.; Nikonova, A. Y.; Antina, Y. V.; Berezin, M. B.; Vyugin, A. I. Synthesis, Spectral-Luminescent Properties, and Photostability of Zn(II) Complexes With Dipyrrins Modified by the Periphery and Meso-Spacer. *Chem. Heterocycl. Compd.* **2014**, *49*, 1740–1747.

(40) Swinehart, D. F. The Beer-Lambert Law. *J. Chem. Educ.* **1962**, *39*, 333.

(41) Suzuki, K.; Kobayashi, A.; Kaneko, S.; Takehira, K.; Yoshihara, T.; Ishida, H.; Shiina, Y.; Oishi, S.; Tobita, S. Reevaluation of Absolute Luminescence Quantum Yields of Standard Solutions Using a Spectrometer with an Integrating Sphere and a Back-Thinned CCD Detector. *Phys. Chem. Chem. Phys.* **2009**, *11*, 9850.

(42) Montalti, M.; Credi, A.; Prodi, L.; Gandolfi, M. T. *Handbook of Photochemistry, Third Edition*; CRC press, 2006.

(43) Demasa, J. N.; Crosby, G. A. The Measurement of Photoluminescence Quantum Yields.1 A Review2. *J. Phys. Chem.* **1971**, *75*, 991–1024.

(44) Bensasson, R.; Land, E. J. *A General Method for Measuring Triplet—Triplet Extinction Coefficients, Singlet—Triplet Intersystem Crossing Efficiencies, and Related Parameters*; Springer: Boston, MA, 1978.

(45) Bensasson, R.; Amand, B. Determination of Triplet Quantum Yields by Laser Flash Absorption Spectroscopy. *Chem. Phys. Lett.* **1975**, *34*, 48–44.

(46) Ruthkosky, M.; Castellano, F. N.; Meyer, G. J. Photodriven Electron and Energy Transfer from Copper Phenanthroline Excited States. *Inorg. Chem.* **1996**, *35*, 6406–6412.

(47) Fu, L.; Jiang, F.-L.; Fortin, D.; Harvey, P. D.; Liu, Y. A Reaction-Based Chromogenic and Fluorescent Chemodosimeter for Fluoride Anions. *Chem. Commun.* **2011**, *47*, 5503.

VITA

NORAH ZARIB ALQAHTANI

Education: M.S. Chemistry, East Tennessee State University (ETSU), Johnson City, Tennessee 2018

B.Sc Chemistry, University of Dammam, Dammam, Saudi Arabia 2013

Honor and Awards: Second Class Honors in B.Sc Chemistry